Geochemistry of Lower Eocene Sandstones in the Rocky Mountain Region

GEOLOGICAL SURVEY PROFESSIONAL PAPER 789

Geochemistry of Lower Eocene Sandstones in the Rocky Mountain Region

By JAMES D. VINE *and* ELIZABETH B. TOURTELOT

With a section on DIRECT-READER SPECTROMETRIC ANALYSES

By RAYMOND G. HAVENS *and* ALFRED T. MYERS

GEOLOGICAL SURVEY PROFESSIONAL PAPER 789

A regional study of element distribution, petrology, and diagenesis among samples of fluvial sandstone from basins of Tertiary age in the Rocky Mountain region

UNITED STATES GOVERNMENT PRINTING OFFICE, WASHINGTON : 1973

UNITED STATES DEPARTMENT OF THE INTERIOR

ROGERS C. B. MORTON, *Secretary*

GEOLOGICAL SURVEY

V. E. McKelvey, *Director*

Library of Congress catalog-card No. 72-600317

For sale by the Superintendent of Documents, U.S. Government Printing Office, Washington, D.C. 20402
Price (paper cover) 75 cents domestic postpaid or 55 cents GPO Bookstore Stock Number 2401–00275

CONTENTS

ILLUSTRATIONS

TABLES

GEOCHEMISTRY OF LOWER EOCENE SANDSTONES IN THE ROCKY MOUNTAIN REGION

By JAMES D. VINE and ELIZABETH B. TOURTELOT

ABSTRACT

The composition of lower Eocene fluvial sandstones in the Rocky Mountain region was studied to aid in interpretation of the regional geochemical environment of uranium and other mineral deposits in rocks of early Eocene age. The study was based on 216 samples, from 18 basins, collected according to a hierarchial plan that involved the random selection of three pairs of beds in each of 36 sample areas. The geometric means of the constituents (in percent) and of the minor elements (in parts per million) for these 216 samples are as follows (geometric deviation in parentheses): SiO_2, 72.9 (1.2); Al_2O_3, 6.6 (1.9); total iron as Fe_2O_3, 1.2 (2.1); MgO, 0.6 (3.0); CaO, 2.4 (4.3); Na_2O, 0.5 (4.6); K_2O, 1.4 (2.3); H_2O+, 1.4 (1.6); TiO_2, 0.2 (1.9); P_2O_5, 0.05 (2.6); MnO, 0.06 (2.1); CO_2, 0.7 (12.6); B, 13 (2); Ba, 415 (2); Co, 4 (2); Cr, 13 (3); Cu, 8 (2); Ga, 9 (2); La, 12 (2); Ni, 9 (2); Pb, 8 (2); Sr, 138 (3); V, 24 (2); Y, 10 (2); Zr, 113 (2); U, 2.4 (2); and Th, 4.3 (2).

The sampled rocks include feldspar-rich sandstones, which were derived from the erosion of crystalline rocks, and quartz-rich sandstones and carbonate-rich sandstones, which were derived from reworked older sedimentary strata. Rocks rich in both carbonate and feldspar are classed as intermediate. Feldspar-rich sandstones are characteristic of a broad area of central Wyoming, much of Colorado, and northern New Mexico. Carbonate-rich sandstones are characteristic of a narrow belt through central Utah with extensions in the adjacent States. Intermediate rocks lie between carbonate-rich and feldspar-rich sandstones in western Wyoming and northeastern Utah. Quartz-rich rock was found in one area of the Bighorn Basin of Wyoming.

The data from chemical, X-ray diffraction, and petrographic analyses were analyzed statistically. Principal-component analysis of the correlation matrix was used to identify five geochemical groups—a quartz group, a feldspar group, a carbonate group, and two minor-element groups between the feldspar and carbonate groups. Boron, titanium, and zirconium occur in resistate minerals and correlate poorly with everything else except possibly with quartz. Cobalt, chromium, copper, nickel, and vanadium tend to be associated with the intermediate rocks. The enrichment of uranium tends to correlate with feldspar-rich sandstones.

Statistical analysis of dominantly red, orange, yellow, or green subsets of the samples shows that the dominantly green samples differ significantly from the other subsets and that the greatest difference is between the green and the red subsets. The subset of 11 green sandstones has a greater concentration of mica, cobalt, chromium, copper, nickel, strontium, vanadium, gallium, total iron, titanium, and the feldspars, especially plagioclase, than the average of all samples.

Early diagenetic alteration is evidenced by widespread authigenic clay, carbonate, and zeolite minerals, the etching of quartz, the presumed dissolution of mafic silicate minerals, and the enrichment of minor elements in areas of intermediate rock rather than in areas rich only in feldspar, quartz, or carbonate. In many areas, red sandstone probably represent rocks that were originally greenish gray and that were altered at a later stage. Although rock color can be the result of many processes, the red alteration may have been caused by the introduction of oxygenated meteoric ground waters and the accompanied leaching of iron and many of the more mobile elements.

INTRODUCTION AND ACKNOWLEDGMENTS

Conventional petrologic techniques are combined with the statistical analysis of chemical and mineralogic data in this study to interpret the geochemical history of lower Eocene fluvial sandstones in the Rocky Mountain region. Rocks of Eocene age, including the sandstones which intertongue with or grade into other facies of Eocene sedimentary rocks, contain many diverse and valuable mineral deposits in the same or neighboring basins such as uranium, oil shale, trona, nahcolite, dawsonite, petroleum, phosphate, and gold. Genetic relations between such deposits might be brought out by studying the deposits within the larger framework of the regional geochemical setting. Uranium deposits occur in the Wind River, Shirley, Great Divide, and Powder River Basins (Harshman, 1969); oil-shale deposits, in the Green River, Piceance Creek, and Uinta Basins (and lesser deposits in the Great Divide, Washakie, Fossil, Sand Wash, and Bighorn Basins and the Gunnison Plateau) (Bradley, 1964; Donnell, 1961a; Cashion, 1957, 1967; Culbertson, 1964); trona, in the Green River Basin (Bradley and Eugster, 1969); dawsonite and nahcolite, in the Piceance Creek Basin (Smith and Milton, 1966; Hite and Dyni, 1967); hydrocarbons, including petroleum gilsonite, and other solid bitumens, in parts of the Uinta, Piceance Creek, Green River, and Washakie Basins (Bell and Hunt, 1963; Oil and Gas Journal, 1970); gold, in parts of the Sand Wash, Hoback, and western Wind River Basins (Theobald, 1970; Antweiler and Love,

1967); and uranium-bearing phosphorites, in the Green River Basin (Love, 1964).

The origin and distribution of most of the Eocene uranium deposits are thought to be directly related to the geochemical history of lower Eocene sandstones. The chemical properties of mineralizing fluids trapped within a wedge of sediments were probably affected by different lithologies, from clastic detritus to evaporites. Migration patterns of the fluids were locally complex, and possibly fluids migrated between basins. Therefore, a thorough understanding of the distribution of uranium and other epigenetic mineral deposits depends on some knowledge of the geochemical history of the entire wedge of sediment in each basin. This report deals with only one lithologic facies, the fluvial sandstones, and only the lower part of the total wedge of Eocene sediments. Thus, any conclusions reached are necessarily limited in time and scope, and much additional work remains to be done.

Emphasis has been placed on the compilation of geochemical data for determining the history of alteration and for studying the formation of authigenic minerals and the mobility of minor elements. Evidence for widespread formation of authigenic minerals by either digenesis or hydrothermal alteration was presented in a preliminary report (Vine and Tourtelot, 1970a). Some of the same evidence will be reviewed here, and a more thorough statistical analysis of the chemical and mineralogic data will be given.

To plan and execute a regional project as extensive as this required the advice, stimulation, and direct assistance of many colleagues. We thank Alfred T. Miesch for his help in planning and teaching us the use of the statistical methods that we applied. Geologists of the U.S. Geological Survey who contributed information about the areas to be sampled included William B. Cashion, William C. Culbertson, John R. Donnell, James R. Gill, E. N. Harshman, Ross B. Johnson, William R. Keefer, Thomas E. Mullens, Willis L. Rohrer, William N. Sharp, Paul K. Theobold, Harry A. Tourtelot, and Howard D. Zeller. Richard S. Zeman assisted the senior author in fieldwork during the summer of 1968. We thank Leonard G. Schultz for his advice on making and interpreting the X-ray diffraction analyses. We used a pelletized-sample technique designed by Omer B. Raup for the X-ray analyses. Richard A. Sheppard helped identify laumontite in the X-ray traces and in thin section. Melvin E. Johnson made special plastic-impregnated thin sections of the many friable-sandstone samples. The work of John Moreland in preparing, grinding, and splitting samples and renumbering all samples in a random sequence for submission to the laboratories is much appreciated. Louise S. Hedricks and Richard B. Taylor aided us in preparing the photomicrographs of thin sections. George Van Trump, Robert Terrazas, and others in the computer facility helped us use the computer.

Chemical and spectrometric analyses were performed in the laboratories of the U.S. Geological Survey. Direct-reader spectrometric analyses were done in the Denver laboratory by Nancy Conklin, R. G. Havens, and Lorraine Lee, analysts, under the supervision of A. T. Myers. Total-carbon analyses were made in the Denver laboratory by I. C. Frost, Elsie Rowe, G. D. Shipley, and Winona Wright. The rapid rock analyses were made in the Washington laboratory by Lowell Artis, S. D. Botts, G. W. Chloe, Paul Elmore, J. S. Glenn, James Kelsey, and H. Smith, analysts, under the supervision of Leonard Shapiro. Carl M. Bunker and Charles A. Bush performed the gamma-ray analyses for uranium and thorium. The chemical and mineralogical data were placed on punch cards at the geochemical data storage and retrieval facilities, operated by Raoul V. Mendez and Josephine Boerngen.

GEOLOGIC SETTING

DISTRIBUTION AND PALEOGEOGRAPHY

Eocene sedimentary rocks in the Rocky Mountain region were deposited in intermontane basins separated by tectonically active uplifts resulting from orogenic forces which began in Late Cretaceous time. Potassium-argon radioactive age dates indicate a probable interval of about 5 m.y. (million years) from 54 to 49 m.y. B.P. (before present) for deposits of early Eocene age (Evernden and others, 1964). The composition, distribution, and coarseness of sediments in each basin reflect the composition of rocks in the source terrane and the degree of tectonic activity in the adjacent ranges as well as the tectonic activity and environment of deposition within the basin. Some uplifts, such as the fold belt in western Wyoming and adjacent parts of Utah and Idaho, consisted chiefly of Paleozoic and Mesozoic sedimentary rocks. Detritus shed from these ranges included the disintegration products of limestone, dolomite, chert, shale, and sandstone. Precambrian crystalline rocks were exposed in the Bighorn Mountains, Wind River Range, and Laramie Mountains of Wyoming and the Medicine Bow Mountains and Park Range of Colorado. These ranges contributed much arkosic material beginning at about the start of the Eocene. The Precambrian core at the eastern end of the Uinta Mountains was probably also exposed by earliest Eocene time (Culbertson, 1969), but there the Precambrian consisted of quartz-rich sedimentary rocks. Some basins were partly surrounded by

mountain ranges that consisted of rocks of widely different compositions, and so a great variety of detritus was deposited simultaneously in the same basin. Figure 1 shows the distribution of depositional basins in the Rocky Mountain region in early Eocene time and the major uplifts that were important contributors of sediment to the basins. Low interbasin divides that contributed little or no sediment are not shown. Some other basins, such as North Park, Colo., may have been receiving sediments at that time, but since then any such sediments either have been eroded away or have been completely buried by younger sediments.

Fanglomerates and diamictite facies (Tracey and others, 1961) formed adjacent to rapidly rising mountains. Basinward, the coarse facies grade into fluvial sandstones and mudstones and, locally, claystones, algal limestones, carbonaceous shales, and coal beds. Coal beds are numerous in the Powder River, Great Divide, and Hanna basins and are sparse to absent in the other basins. Swamps and lakes began to form in the central parts of some of the basins early in Eocene time. The resultant paludal and lacustrine sediments interfinger with the fluvial lower Eocene sediments (Bradley, 1964; Roehler, 1965) of this study. A warm, mild climate is inferred from numerous studies of fossil plants and vertebrates (Barghoorn, 1953; Bradley, 1963; Van Houten, 1948; Soister, 1968, p. A44).

About middle Eocene time the basins became filled with sediment. Ponds and lakes expanded, and some former low divides were buried by sediment deposited in giant lakes such as Lake Gosiute (Bradley, 1964, fig. 10, p. A36) in southwestern Wyoming. Elsewhere, low divides were buried by fluvial sediment spreading from adjacent basins. Probably, interfingering fluvial and lacustrine sediment in the Hoback, Green River, Fossil, Great Divide, Washakie, and Sand Wash basins formed a continuous deposit.

Middle Eocene volcanic sediments occur in both the lake-bed and fluvial sediments. Toward late Eocene time the lakes grew smaller and disappeared, and the fluvial sediments of that time contain much volcanic debris. Periodic minor downwarp and uplift reestablished some low divides.

In some basins, folding and faulting occurred at the end of early Eocene time and was renewed periodically during later Tertiary time, but in the Wind River Basin, as noted by Keefer (1970, p. D9), "with few exceptions these movements were of minor consequence and did not greatly modify the structural patterns that had already been established." Many of the basins continued to fill throughout most of Tertiary time (Love, 1970, p. C111–C123) until only a few of the highest mountain peaks extended above the general basin fill. Sedimentation ceased at different times from basin to basin, but in general the present major cycle of exhumation and downcutting probably began in Miocene or Pliocene time.

Early Eocene sedimentation rates were moderately rapid to rapid in most basins of the Rocky Mountain region, ranging from about 500 to 5,000 feet in 5 m.y. These compare with Late Cretaceous sedimentation rates of from 60 feet per m.y. in central North and South Dakota to as much as 2,500 feet per m.y. locally in western Wyoming, according to J. R. Gill (oral commun., 1971). The Eocene sedimentation was sufficiently rapid that many unstable minerals, including feldspars, clay minerals, and mafic minerals, probably arrived at the site of deposition without much chemical alteration. The resulting sediments include mineral constituents that have not had time to come into chemical equilibrium with each other or with the enclosing pore waters.

The lower Eocene sedimentary rocks were exposed (fig. 1) by late Cenozoic time at the margins of most basins or areas of preservation. The largest volumes of lower Eocene strata are preserved in the large basins such as the Green River, Wind River, and Powder River basins of Wyoming, but smaller deposits of lower Eocene strata are also preserved in other structural settings. The Wasatch Range and Wasatch Plateau areas of Utah contain Eocene strata preserved in uplifted mountain blocks, and the Galisteo basin of New Mexico contains Eocene rocks preserved in several isolated downfaulted blocks. The paleogeographic setting is most easily reconstructed for the basin areas and is difficult or impossible to reconstruct for the other areas.

Although our original intention was to study sandstones representing fluvial deposition, we were unable to distinguish among stream-channel sandstones, flood plains, alluvial fans, pediments, debris flows, and perhaps even paludal, dune, and beach deposits. Truly lacustrine sandstones, as recognized by horizontal lamination, much fossil shell debris, or well-rounded and well-sorted grains, were excluded.

STRATIGRAPHIC RELATIONS

Though different stratigraphic names have been applied to lower Eocene sedimentary rocks in different basins, the history of sedimentation is very similar throughout the region. In most basin areas, especially in Wyoming, sedimentation was continuous from latest Cretaceous to middle or late Tertiary time except for local interruptions in late Eocene time (Love and others, 1963). Unconformities occur locally at or near the base of Eocene strata along

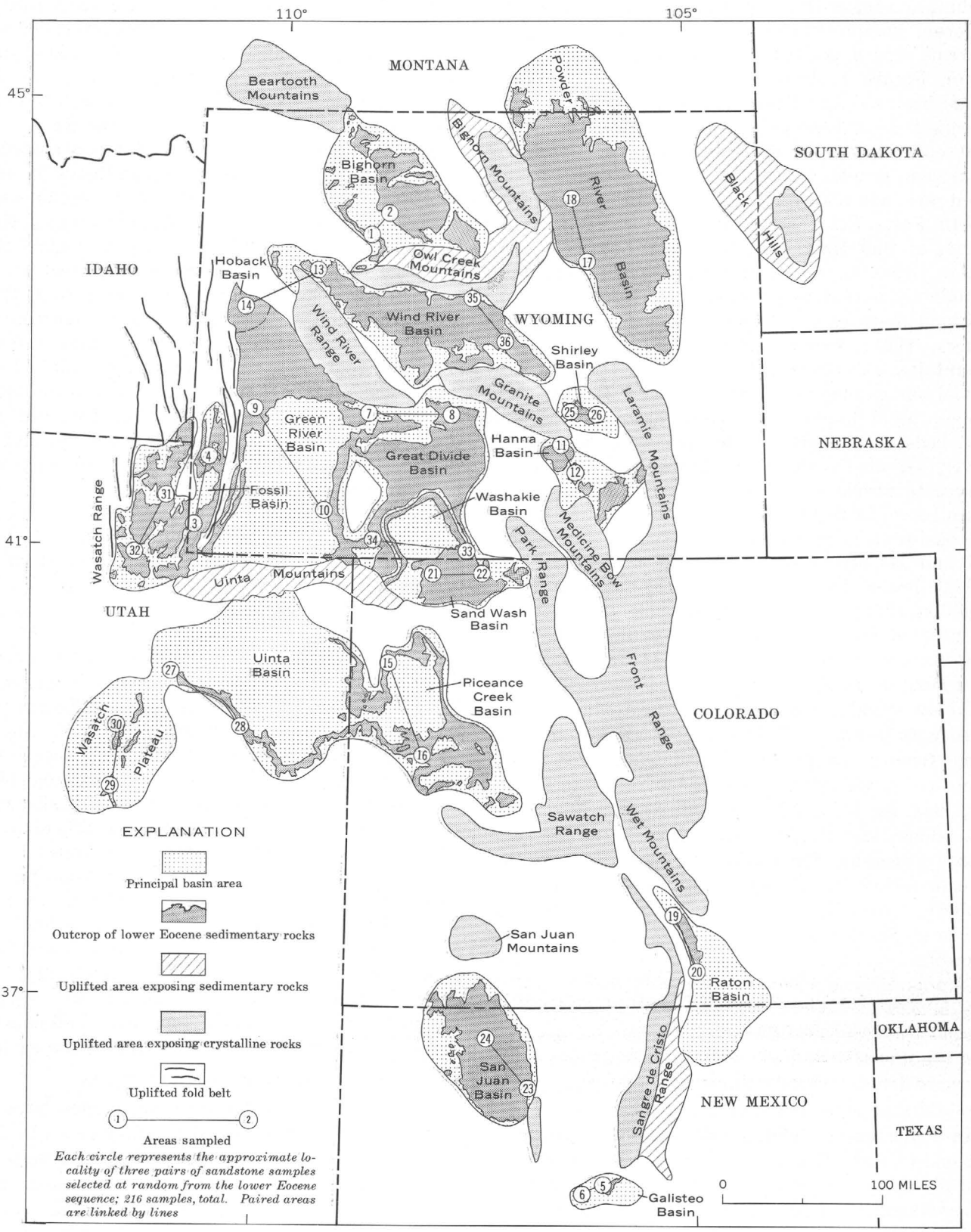

FIGURE 1. — Basins and major uplifts in early Eocene time, present outcrop pattern of lower Eocene sedimentary rocks, and sample localities. Interbasin divides that did not contribute much debris are not shown. Basins and major uplifts modified from King (1959, figs. 66, 69). Present outcrop pattern compiled from various sources, including State geologic maps.

Sample localities shown in figure 1

1. Enos Creek
2. Hillberry Rim
3. Evanston
4. Fossil
5. Cerrillos
6. Hagen
7. Oregon Buttes
8. Crooks Gap–Wamsutter
9. La Barge
10. Firehole Basin
11. Difficulty
12. Carbon basin
13. Dubois
14. Hoback basin
15. Rangely
16. Battlement Mesa
17. Pine Ridge–Pumpkin Buttes
18. Horse Creek–Crazy Woman Creek
19. Huerfano Park
20. West Spanish Peak
21. Little Snake River
22. Elkhead Mountains
23. Cuba
24. Gobernador
25. Bates Hole
26. Chalk Hills
27. Soldier Summit
28. Patmos Head
29. Salina
30. Gunnison Plateau
31. Woodruff
32. Morgan
33. Baggs
34. Erickson–Kent Ranch
35. Lost Cabin
36. Wallace Creek

the basin margins, but deposition was probably continuous near the center of each basin, perhaps only a few miles distant (fig. 2).

In parts of southwestern Wyoming, abundant mammal fossils allow precise dating of strata (Gazin, 1962). However, in many other areas fossils are lacking or are not diagnostic. In mapping, an arbitrary boundary between Paleocene and Eocene strata is commonly defined on the basis of subtle changes in color, texture, or composition of the rocks. In many areas, Eocene rocks tend to be more brightly colored than Paleocene rocks; red, green, and purple mudstones are characteristic of the lower Eocene strata, whereas drab shades of brown and gray characterize mudstones in the Paleocene strata. The lowest arkosic sandstones form a mappable boundary for the base of the Eocene in some parts of Wyoming according to N. M. Denson (oral commun., 1970). Color, texture, and rock composition are all unreliable indicators of age, however, and within the Rocky Mountain region the exact placement of the boundary between Paleocene and Eocene strata in

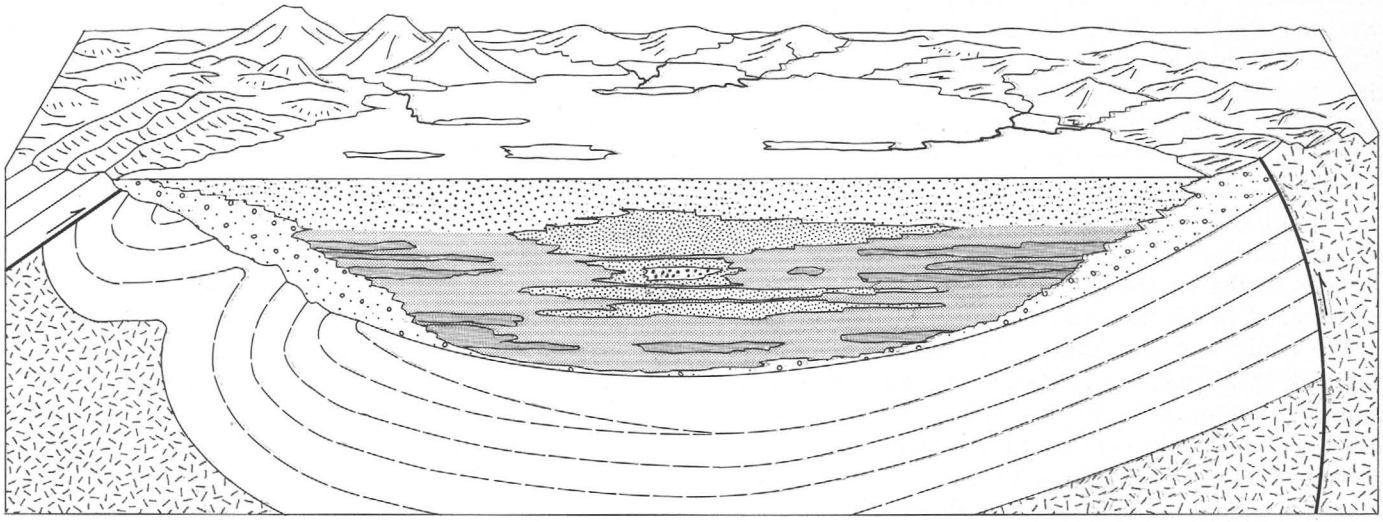

EXPLANATION

Upper and middle Eocene fluvial sediments

Lacustrine and evaporite sediments

Lower Eocene fluvial mudstone and sandstone

Lower Eocene conglomerates and diamictites

Pre-Eocene sedimentary rocks

Precambrian crystalline rocks

Geologic boundary
Dashed where gradational

Fault
Arrow shows upthrown side

FIGURE 2. — Generalized cross section of an Eocene basin at the end of the Eocene Epoch. Modified from Bradley (1964).

490-247 O - 73 - 2

any specific area is often disputed among paleobotanists, vertebrate paleontologists, invertebrate paleontologists, and physical stratigraphers. Not uncommonly the boundary based on paleontological criteria is within a lithostratigraphic unit.

Whereas the lower boundary of the lower Eocene strata is locally unconformable and is generally based on paleontologic evidence, the upper boundary is nearly everywhere conformable and is based on a lithologic change supplemented by meager fossil data. Throughout western Wyoming, northwestern Colorado, and northeastern Utah, the lower Eocene fluvial strata intertongue with and are overlain by lacustrine strata. The upper boundary of the strata included in this study is not a time-stratigraphic boundary but is a boundary between fluvial and lacustrine rocks in the Uinta, Piceance Creek, Green River, Sand Wash, Fossil, Washakie, Great Divide, and central Bighorn Basins and in the Wasatch Plateau. A lithologic change from dominantly detrital to dominantly volcanogenic sediments marks approximately the same stratigraphic positions in the western Bighorn, Wind River, and Shirley Basins. Other lithologic changes are recognized in the northern Raton and Hoback basins. Middle or upper Eocene rocks have not been reported from the Hanna, San Juan, or Powder River Basins. The boundary between lower and middle Eocene rocks was arbitrarily placed on the basis of meager fossil evidence, as one-third of the distance above the base of the Eocene rocks in the Galisteo basin. No stages are recognized in the Wasatch Range.

We could not find thoroughly documented or described stratigraphic sections of the rocks to be sampled for each basin. We relied as much as possible on published reports of the presence of early Eocene fossils or on physical evidence that the rocks sampled could be correlated with strata that were reported to contain early Eocene fossils. Table 1 lists the areas where sandstone was sampled, principal references to a stratigraphic section described in each area, and petrographic descriptions. Most stratigraphic thicknesses in the table are quoted directly from the cited reference, but we estimated the thickness at some places, as indicated in the table. Where a range in thickness is given, the stratigraphic unit was generally sampled near the area where it is thickest. Where a minimum thickness is given, the complete thickness may be unknown because of poor exposures or because the top has been eroded away. Where two thicknesses are separated by a comma, the fluvial sequence is divided into two tongues which are separated by an unspecified thickness of lacustrine strata. Plant microfossils recently described by Gill, Merewether, and Cobban (1970, p. 47–48) suggest that the lowermost samples we collected from the Carbon basin may be late Paleocene rather than early Eocene in age.

SAMPLING PLAN

The sample population for this study consists of those accessible lower Eocene fluvial sandstones exposed in the Rocky Mountain region (fig. 1) that are not conspicuously weathered, mineralized, or metamorphosed. We recognize that all sandstone included in the sample population have been weathered to some degree and have been diagenetically altered during their 50 m.y. history; these processes have contributed to their present geochemical character.

The object of the sampling plan was to obtain unbiased geochemical information about the sample population. The sampling plan was designed so that statistical techniques could be used to look for geographic patterns in the distribution of individual constituents and to determine the characteristics of the target population. We hope that the sampling plan would be such that the characteristics of the lower Eocene fluvial sandstones could be determined and that the effect of microenvironments within the fluvial sedimentation regime could be minimized. Sampling was also limited by the amounts of time and money available for field and analytical work as well as by natural conditions such as the accessibility and abundance of suitable outcrops.

We designed a four-level hierarchial sampling plan similar to the plans used by Olson and Potter (1954) and Krumbein and Slack (1956), who described in detail the implications, applications, and theory of hierarchial sampling plans. One major difference between the cited sampling plans and the one used in this study is that the cited plans were based on predetermined geographic spacing between samples, whereas this plan is based on the structural pattern of the region sampled, and the geographic distance between sample localities varies greatly (fig. 1). The design of the sampling plan used in this study is as follows:

Level 4: The 18 major basins of lower Eocene deposition within the Rocky Mountain region;[1]

Level 3: Two areas, or stratigraphic sections, within each major basin of deposition;

Level 2: A set consisting of three pairs of sandstone beds within each stratigraphic section; and

Level 1: A pair of sandstone beds, each represented by one sample.

[1]The original sampling plan included two areas (12 samples) from the Bearpaw Mountains of north-central Montana. Analysis of these samples showed that some contained authigenic amphibole, indicating a higher degree of metamorphism than we thought acceptable for this study. Data from these samples were included, however, in a preliminary report (Vine and Tourtelot, 1970a).

TABLE 1.—*Sample localities, stratigraphic assignments, and petrographic descriptions of 216 samples of lower Eocene sandstone*

[An asterisk (*) preceding the thickness indicates our estimate. The four color subsets represent a compilation of the following colors from the "Rock-Color Chart" of Goddard and others (1948): Red, 10*R* 6/2, 10*R* 6/6, 10*R* 7/4, 7*R* 7/4, 10*R* 5/4, 5*YR* 8/1, 5*YR* 7/2, 5*YR* 8/4, and 5*R* 8/1; orange, 10*YR* 8/2, 10*YR* 7/4, 10*YR* 8/6, 10*YR* 7/6, 10*YR* 6/4, 5*YR* 4/1, 5*YR* 5/6, and 5*YR* 6/4; yellow, 5*Y* 7/2, 5*Y* 8/1, 5*Y* 8/4, 5*YR* 6/1, *N* 8, and *N* 9; and green, 5*Y* 7/1, 5*Y* 6/1, 5*Y* 5/2, 5*GY* 7/2, 5*GY* 8/1, 5*G* 8/1, and 10*Y* 8/2. Petrographic descriptions are based on thin-section study, supplemented by field descriptions, X-ray diffraction data, and a few heavy mineral studies]

Locality No. (figs. 1, 5)	Area and reference	Stratigraphic unit; thickness (ft)	Field sample No.	Locality: Sec., T. and R.	Number of samples in specified color subset	Petrographic description
			Bighorn Basin, Wyo.			
1	Enos Creek (Rohrer, 1966).	Willwood Formation; 340.	BH07–BH12	NE¼ 28 46 N., 100 W.	5 orange, 1 yellow.	Very poorly to poorly sorted, very fine to coarse-grained. Quartz, microcline, fresh to altered plagioclase, chert, and composite grains in clay or carbonate matrix; some iron stain. Accessory minerals: white mica, fresh to very altered green and brown biotite, chloritoidlike minerals, zircon, garnet, tourmaline, glauconite, and opaque minerals.
2	Hillberry Rim (Van Houten, 1944).	Willwood Formation; *600.	BH01–BH06	N½ 1 47 N., 99 W.	4 orange, 2 yellow.	Poorly sorted, very fine to medium-grained. Quartz, chert, potassium feldspar, sparse plagioclase, and clay closely packed in clay matrix; some iron stain. Accessory minerals: fresh to altered biotite, zircon, tourmaline, hypersthene, glauconite, and opaque minerals.
			Fossil Basin, Wyo.			
3	Evanston (Oriel and Tracey, 1970).	Wasatch Formation; 1,000–1,500.	FO01–FO06	22 15 N., 119 W.	5 yellow, 1 orange.	Poorly sorted, very fine to very coarse grained. Quartz, chert, fresh to altered feldspars (chiefly potassium feldspars), composite grains, schist, sedimentary rock fragments, and calcite and dolomite grains in carbonate matrix. Accessory minerals: white mica, green biotite, zircon, garnet, epidote, chlorite, and opaque minerals.
4	Fossil (Oriel and Tracey, 1970).	Wasatch Formation; 1,000–1,500.	FO07–FO12	SE¼ 26 22 N., 118 W.	4 yellow, 2 orange.	Very poorly to poorly sorted, medium to very coarse grained. Quartz, chert, dolomite rhombs, and sparse feldspars in carbonate and clay matrix; some iron stain. Accessory minerals: zircon; few accessory minerals present.
			Galisteo Basin, N. Mex.			
5	Cerrillos (Robinson, 1957).	Galisteo Formation, lower part; 930.	GA01–GA06	SE¼ 16 14 N., 8 E.	4 red, 1 orange, 1 yellow.	Very poorly to poorly sorted, medium to very coarse grained. Quartz, chert, generally fresh feldspars, composite grains, and carbonate grains in clay or calcite matrix. Accessory minerals: white mica, zircon, tourmaline, garnet, opaque minerals; few accessory minerals present.
6	Hagen (Stearns, 1943).	Galisteo Formation, lower part; 1,270.	GA07–GA12	27 13 N., 6 E.	2 red, 2 orange, 2 yellow.	Poorly to moderately well sorted, fine- to coarse-grained. Quartz, fresh to completely altered feldspars, chert, and schist closely packed to floating in clay matrix, sparse calcite matrix; some iron stain. Accessory minerals: fresh to altered brown and green biotite, epidote, garnet, zircon, clinozoisite, and opaque minerals.
			Great Divide Basin, Wyo.			
7	Oregon Buttes (Zeller and Stephens, 1969).	Wasatch Formation, main body; 3,000.	GD01–GD02	9 24 N., 99 W.	2 yellow.	Poorly sorted, fine- to medium-grained. Quartz, chert, fresh to altered feldspars, dolomite, and detrital calcite in clayey calcite matrix. Accessory minerals: fresh to altered biotite, chlorite, garnet, zircon, tourmaline, epidote, zeolite, and opaque minerals.
		Wasatch Formation, Cathedral Bluffs Tongue; 160–200.	GD03–GD06	S½ 21 27 N., 101 W.	2 green, 2 yellow.	Very poorly sorted, granular to conglomeratic. GD03 and GD04 too friable for thin section. Quartz, fresh to completely altered feldspars, schist, and sandstone fragments in calcite and chlorite matrix. Accessory minerals: abundant muscovite and biotite, authigenic epidote, chlorite, garnet, zircon, and opaque minerals.
8	Crooks Gap–Wamsutter (Stephens, 1964; Masursky, 1962).	Battle Spring Formation; 500–2,500.	GD07–GD08	NW¼ 19 27 N., 92 W.	2 yellow.	Very poorly sorted, granular. GD07 too friable for thin section. Microcline, fresh to altered plagioclase, and quartz in sparse clay matrix. Accessory minerals: altered green and brown biotite; few accessory minerals present.
			GD09–GD10	2 26 N., 93 W.	do.	Poorly sorted, coarse-grained. Etched quartz and altered feldspars in clay or calcite matrix. Accessory minerals: altered biotite; very few accessory minerals.
		Wasatch Formation; 500–3,500.	GD11–GD12	22 22 N., 94 W.	1 yellow, 1 green.	Poorly to moderately well sorted, very fine to medium-grained. Quartz, fresh to altered feldspars, detrital dolomite, limestone, and shale grains in iron-stained clay matrix. Accessory minerals: altered biotite, white mica, garnet, zircon, tourmaline, epidote, chlorite, and opaque minerals.
			Green River Basin, Wyo.			
9	La Barge (Oriel, 1961, 1962; Privrasky, 1963).	Wasatch Formation, New Fork Tongue; 250.	BB07–BB10	9 27 N., 113 W.	4 green.	Poorly sorted, very fine to medium-grained. BB07–BB09: Quartz, carbonate grains, fresh to altered feldspars, and analcime tightly packed in very little clay matrix. Accessory minerals: abundant green, red, and brown biotite, garnet, zircon, and opaque minerals. BB10: strongly etched quartz and feldspars in carbonate matrix. Accessory minerals: biotite, garnet, zircon, tourmaline, anhydrite, and opaque minerals.

TABLE 1. — *Sample localities, stratigraphic assignments, and petrographic descriptions of 216 samples of lower Eocene sandstone*—Continued

Locality No. (figs. 1, 5)	Area and reference	Stratigraphic unit; thickness (ft)	Field sample No.	Locality: Sec., T. and R.	Number of samples in specified color subset	Petrographic description
			Green River Basin, Wyo. — Continued			
		Wasatch Formation, main body; *1,500.	BB11–BB12	9 27 N., 113 W.	2 orange.	Poorly sorted, fine- to coarse-grained. Quartz, fresh to altered feldspars, chert, and mica schist in iron-stained carbonate matrix. Accessory minerals: abundant biotite, muscovite, clay, dolomite, garnet, tourmaline, epidote, and zircon.
10	Firehole Basin (Culbertson, 1965).	Wasatch Formation, main body; 2,400.	BB01–BB04	34 17 N., 106 W.	2 yellow, 1 red, 1 orange.	Poorly to moderately well sorted, very fine to medium-grained. BB01–BB02: quartz, fresh to altered feldspars, chert, and dolomite in iron-stained clayey carbonate matrix. Accessory minerals: fresh to altered green and brown biotite, white mica, garnet, zircon, tourmaline, and chloritoidlike minerals. BB03–BB04: quartz, feldspars which are altered to sericite or analcime, dolomite grains with iron-stained rims, chert, and schist in clay matrix. Accessory minerals: fresh to altered biotite, chlorite, abundant garnet (as large as 5 mm), white mica, epidote, blue and green tourmaline, and opaque minerals.
		Wasatch Formation, Niland Tongue; 450.	BB05–BB06	SW¼ 34 17 N., 106 W.	2 yellow.	Poorly to moderately well sorted, fine- to medium-grained. Etched quartz, fresh to altered feldspars, schist, and dolomite closely packed to floating in calcite and clay matrix. Accessory minerals: red, green, and brown biotite, chlorite, white mica, coarse garnets, epidote, tourmaline, and opaque minerals.
			Hanna Basin, Wyo.			
11	Difficulty (Knight, 1951; Gill, 1970, p. 47–48).	Unnamed Eocene rocks; 1,500.	HN01–HN04	NW¼ 26 24 N., 81 W.	3 yellow, 1 orange.	Very poorly to poorly sorted, fine-grained to conglomeratic. HN01 too friable for thin section. Quartz, fresh to altered feldspars, composite grains, and clay aggregates in clay matrix; some iron stain. Accessory minerals: fresh to altered biotite, chloritoidlike minerals, zircon, tourmaline, epidote, and opaque minerals; accessory minerals sparse.
			HN05–HN06	SW¼ 23 24 N., 81 W.	1 yellow, 1 orange.	Very poorly to poorly sorted, medium-grained to granular. Composite grains of quartz and feldspar, quartz, and fresh to altered feldspars in clay and calcite matrix. Accessory minerals: fresh to altered green and brown biotite, white mica, zircon, nephrite, chlorite, and opaque minerals; accessory minerals sparse.
12	Carbon basin (Dobbin and others, 1929).	Unnamed Eocene rocks and rocks of probable Paleocene age mapped as Hanna Formation; 7,000.	CA01–CA04	SE¼ 20 21 N., 79 W.	2 orange, 1 red, 1 yellow.	Poorly sorted, fine-grained. Quartz, chert, feldspars, schist, and dolomite rhombs densely packed to floating in clay and carbonate matrix; some iron stain. Accessory minerals: altered biotite, white mica, chlorite, zircon, garnet, tourmaline, and opaque minerals.
			CA05	SW¼ 24 21 N., 79 W.	1 yellow.	Poorly sorted, medium-grained. Quartz, fresh to altered feldspars, and chert in calcite matrix. Accessory minerals: fresh to altered biotite, garnet, tourmaline, zircon, rutile, epidote, and opaque minerals.
			CA06	NW¼ 25 21 N., 79 W.	1 yellow.	Poorly sorted, coarse-grained. Etched quartz, altered feldspars, and chert floating in calcite matrix. Accessory minerals: abundant altered biotite, authigenic epidote, garnet, zircon, tourmaline, and opaque minerals; accessory minerals abundant.
			Hoback–western Wind River Basins, Wyo.			
13	Dubois (Keefer, 1957).	Indian Meadows and Wind River Formations, undivided; 0–1,800.	WR01–WR06	NW¼ 5 41 N., 106 W. SE¼ 32; SE¼ 20 42 N., 106 W.	6 yellow.	Very poorly to poorly sorted, fine to very coarse grained. WR04–WR06 too friable for thin section. Quartz, fresh to altered feldspars, and carbonate grains in carbonate and clay matrix. Accessory minerals: fresh to very altered green and brown biotite, chloritoidlike minerals, garnet, zircon, tourmaline, glauconite, and opaque minerals.
14	Hoback basin (Dorr, 1952).	Hoback Formation, upper part; 3,000.	HO01–HO02	28 38 N., 113 W.	1 orange, 1 yellow.	Poorly sorted, fine- to medium-grained. Quartz, chert, detrital calcite and dolomite, and minor feldspar in carbonate and clay matrix. Accessory minerals: altered biotite, tourmaline, zircon, and opaque minerals; accessory minerals sparse.
			HO03–HO04	NW¼ 34 38 N., 113 W.	1 green, 1 yellow.	Poorly sorted, very fine to coarse-grained. Quartz, chert, fresh to altered feldspars, and detrital carbonate grains closely packed in clay and carbonate matrix. Accessory minerals: abundant biotite, garnet, zircon, white mica, and opaque minerals. HO04 contains several pollen grains or spores.
			HO05–HO06	19 37 N., 113 W.	1 yellow, 1 orange.	Poorly to moderately well sorted, medium- to coarse-grained. Quartz, fresh to altered feldspars, and chert in closely packed clay (HO05) and calcite (HO06) matrix. Accessory minerals: fresh to altered biotite, garnet, sphene, epidote, monazite, zircon, zoisite, and opaque minerals; accessory minerals abundant.
			Piceance Creek basin, Colo.			
15	Rangely (Donnell, 1961a).	Wasatch Formation; 375–580.	PC01–PC04	10 1 N., 100 W.	3 orange, 1 yellow.	Poorly sorted, medium-grained. Quartz, generally altered feldspars, chert, dolomite grains, and

TABLE 1. — *Sample localities, stratigraphic assignments, and petrographic descriptions of 216 samples of lower Eocene sandstone*—Continued

Locality No. (figs. 1, 5)	Area and reference	Stratigraphic unit; thickness (ft)	Field sample No.	Locality: Sec., T. and R.	Number of samples in specified color subset	Petrographic description
			Piceance Creek basin, Colo. — Continued			
						kaolinite closely packed in clay and calcite matrix. Accessory minerals: fresh to altered biotite, garnet, zircon, glauconite, tourmaline, and altered mafic minerals.
			PC05–PC06	10 1 N., 100 W.	2 orange.	Poorly to moderately well sorted, fine-grained. Quartz, feldspars, limestone, and dolomite grains closely packed in calcite matrix; PC06 very iron stained. Accessory minerals: zircon, glauconite, chloritoidlike minerals and opaque minerals; accessory minerals sparse.
16	Battlement Mesa (Donnell, 1961b).	Wasatch Formation; 2,110.	PC07–PC10	SW¼ 30 9 S., 96 W.	2 orange, 2 yellow.	Poorly sorted, fine- to coarse-grained. Quartz, fresh to completely altered feldspars, kaolinite, chert, and limestone grains in iron-stained clay and sparse calcite matrix; birefringent rim of clay around many grains. Accessory minerals: very altered biotite, white mica, zircon, chlorite, and opaque minerals; accessory minerals sparse.
			PC11–PC12	SE¼ 25 9 S., 97 W.	1 red, 1 yellow.	Very poorly to poorly sorted, fine- to coarse-grained. Quartz, fresh to altered feldspar, kaolinite, and chert in clay matrix; birefringent rim of clay around many grains. Accessory minerals: very altered biotite, white mica, zircon, tourmaline, and opaque minerals; accessory minerals sparse.
			Powder River Basin, Wyo.			
17	Pine Ridge–Pumpkin Buttes (Sharp and others, 1964).	Wasatch Formation; 1,575.	PR01–PR04	E½ 12 42 N., 78 W. SE¼ 34 43 N., 78 W.	2 red, 2 yellow.	Very poorly to moderately well sorted, very fine to medium-grained. Quartz, chert, and sparse potassium feldspar in sparse clay matrix. Accessory minerals: white mica, fresh green and blue hornblende, pyroxenes, zircon, tourmaline, epidote, and opaque minerals.
			PR05–PR06	SW¼ 13 44 N., 76 W.	1 orange, 1 yellow.	Poorly sorted, coarse-grained. Too friable for thin section. PR05 contains heulandite.
18	Horse Creek–Crazy Woman Creek (Olive, 1957; Hose, 1955).	Wasatch Formation; 150, 200.	PR07–PR08	23 54 N., 74 W.	1 orange, 1 yellow.	Poorly sorted, fine-grained. Deeply etched quartz and sparse feldspar and dolomite rhombs floating in calcite matrix. Accessory minerals: bright-green and brown biotite, white mica, zircon, garnet, pyroxene, and altered mafic grains.
			PR09–PR12	7 49 N., 79 W. NE¼ 11 49 N., 80 W.	4 yellow.	Poorly sorted, very fine to medium-grained. Etched quartz, chert, and sparse feldspar in abundant calcite matrix. Accessory minerals: brown, yellow, and green biotite, white mica, zircon, garnet, epidote, glauconite, tourmaline, and opaque minerals.
			Raton basin, Colo.			
19	Huerfano Park (Johnson, 1959).	Cuchara Formation; 1,400.	RA07–RA08	7 26 S., 70 W.	1 red, 1 yellow.	Very poorly sorted, coarse-grained to granular. Quartz, feldspars, and schist grains closely packed in sparse calcite matrix. Accessory minerals: altered biotite and opaque minerals; accessory minerals sparse.
		Huerfano Formation; 2,000.	RA09–RA12	SW¼ 17 and 31 26 S., 70 W.	4 red.	Poorly sorted, coarse-grained to granular. Quartz, feldspars (abundant microcline), mica schist, and chert in clay matrix. Accessory minerals: brown biotite, garnet, epidote, and opaque minerals.
20	West Spanish Peak (Johnson and others, 1958).	Huerfano Formation; 2,000.	RA01–RA04	21 31 S., 68 W.	4 red.	Poorly sorted, medium to very coarse grained. Quartz and fresh to altered feldspars in clay and laumontite matrix; laumontite replaces some of matrix and some plagioclase. Accessory minerals: authigenic epidote, garnet, zircon, and opaque grains.
		Cuchara Formation; 400.	RA05–RA06	SW¼ 23 31 S., 68 W.	2 orange.	Poorly sorted, medium to very coarse grained. Quartz and feldspars in clay and laumontite matrix; laumontite replaces some plagioclase. Accessory minerals: altered biotite, authigenic epidote, garnet, and opaque minerals.
			Sand Wash basin, Colo.			
21	Little Snake River (Sears and Bradley, 1924; Theobald, 1970).	Wasatch Formation; >1,500.	SW01–SW02	SE¼ 30 11 N., 94 W.	1 orange, 1 yellow.	Poorly to moderately well sorted, fine- to coarse-grained. SW02–SW05 too friable for thin section. SW01: Quartz and fresh to altered feldspars in clay and iron oxide matrix. Accessory minerals: fresh to altered biotite and white mica, epidote, zircon, garnet, and opaque grains. SW06: Quartz, fresh to altered feldspars and composite grains floating in calcite matrix. Accessory grains: biotite, white mica, and opaque minerals; other accessory minerals contained in framework grains.
			SW03–SW04	26 and 27 11 N., 95 W.	2 yellow.	
			SW05–SW06	12 11 N., 96 W.	1 yellow, 1 orange.	
22	Elkhead Mountains (McKenna, 1960; Theobald, 1970).	Wasatch Formation; >1,500.	SW07–SW08	SW¼ 8 10 N., 88 W.	2 yellow.	Poorly sorted, medium- to coarse-grained. SW07 too friable for thin section. Quartz, fresh to altered feldspars, chert, and shale in clay matrix; rims of clay around grains. Accessory minerals: white mica, zircon, and opaque minerals.
			SW09–SW10	26 11 N., 90 W.	2 yellow.	Poorly to moderately well sorted, fine- to coarse-grained. Quartz, chert, potassium feldspar, and shale in clay matrix; rims of clay around many grains. Accessory minerals: green biotite, white mica, zircon, chloritoidlike minerals, and opaque minerals.

TABLE 1. — *Sample localities, stratigraphic assignments, and petrographic descriptions of 216 samples of lower Eocene sandstone*—Continued

Locality No. (figs. 1, 5)	Area and reference	Stratigraphic unit; thickness (ft)	Field sample No.	Locality: Sec., T. and R.	Number of samples in specified color subset	Petrographic description
			Sand Wash basin, Colo. — Continued			
			SW11–SW12	7 11 N., 90 W.	2 orange.	Poorly sorted, fine-grained to conglomeratic. SW12 too friable for thin section. Quartz, fresh to altered feldspars, shale, and chert in sparse clay matrix. SW12 contains gypsum. Accessory minerals: altered biotite, authigenic epidote, garnet, zircon, and opaque minerals.
			San Juan Basin, N. Mex.			
23	Cuba (Baltz, 1967).	San Jose Formation, Llaves Member; 1,300.	SJ01–SJ02	NW¼SE¼ 36 24 N., 1 W.	1 orange, 1 red.	Very poorly to poorly sorted, medium- to coarse-grained. Many composite grains, quartz, chert, fresh to altered feldspars, and schist in clay matrix. Accessory minerals: white mica, biotite, tourmaline, zircon, garnet, apatite, and opaque minerals.
		San Jose Formation, Cuba Mesa Member, upper tongue; 70.	SJ03	SW¼ 31 25 N., 1 E.	1 yellow.	Poorly sorted, medium-grained. Quartz, feldspars, and garnet schist in clay matrix. Accessory minerals: biotite, muscovite, garnet, zircon, chloritoidlike minerals, and opaque minerals.
		San Jose Formation, Regina Member; 726.	SJ04	SW¼ 31 25 N., 1 E.	1 orange.	Moderately well sorted, coarse-grained. Quartz, potassium feldspar, chert, and rare plagioclase closely packed in clay matrix. Accessory minerals: zircon and opaque minerals.
		San Jose Formation, Cuba Mesa Member, upper tongue; 52.	SJ05–SJ06	SW¼ 1 21 N., 2 W.	2 orange.	Poorly sorted, coarse-grained. Quartz, fresh to altered feldspars, chert, schist, and sandstone and shale fragments in sparse clay matrix. Accessory minerals: muscovite, fresh to altered biotite, zircon, chlorite, and opaque minerals.
24	Gobernador (Simpson, 1948).	San Jose Formation; >1,000.	SJ07–SJ12	SE¼ 8 29 N., 4 W.	5 orange, 1 yellow.	Very poorly to moderately well sorted, medium to very coarse grained. Quartz, fresh to altered feldspars, and fragments of igneous, metamorphic, and sedimentary rocks in clay and sparse calcite matrix; some iron stain. Accessory minerals: altered biotite, zircon, white mica, epidote, abundant garnet (especially in SJ12), and opaque minerals.
			Shirley Basin, Wyo.			
25	Bates Hole (Harshman, 1968).	Wind River Formation; 300–400.	SH01–SH02	NW¼ 3 27 N., 80 W.	2 yellow.	Very poorly sorted, medium- to coarse-grained. SH02 too friable for thin section. Coarse quartz and composite grains and fine feldspar grains loosely packed in iron-stained clay matrix. Accessory minerals: altered green biotite, zircon, epidote, wollastonite, monazite, and opaque minerals; accessory minerals abundant.
			SH03–SH06	34 28 N., 80 W.	4 yellow.	Very poorly sorted, granular to conglomeratic. Too friable for thin section.
26	Chalk Hills (Harshman, 1968).	Wind River Formation; 300–400.	SH07–SH12	W½ 16; SE¼ 17 27 N., 77 W.	6 yellow.	Very poorly sorted, very fine to medium-grained. Very friable; thin sections for SH07 and SH08 only: Quartz, fresh to altered feldspars, and composite grains in clay matrix; plagioclase altered to clay. Accessory minerals: white mica, zircon in quartz grains, and opaque minerals; accessory minerals sparse.
			Uinta Basin, Utah			
27	Soldier Summit (Henderson, 1958).	Colton Formation; 1,500.	UI01–UI06	25 11 S., 8 E. SW¼ 23; SW¼ 22 10 S., 7 E.	5 red, 1 yellow.	Very poorly to poorly sorted, very fine to medium-grained. Quartz, altered feldspars, kaolinite, and carbonate grains in clay and carbonate matrix; many grains altered to clay, sericite, and iron oxides. Accessory minerals: white mica, zircon, tourmaline, etched garnet, and opaque minerals.
28	Patmos Head (Fisher and others, 1960).	Wasatch Formation; about *500.	UI07–UI12	N½ 1 16 S., 14 E.	3 orange, 2 red, 1 yellow.	Very poorly to moderately well sorted, very fine to coarse-grained. Quartz, fresh to altered feldspars, chert, and carbonate grains in iron-stained carbonate matrix; sparse clay matrix in UI07. Analcime forms part of matrix and replaces some feldspar grains in all samples except UI07. Accessory minerals: white mica, garnet, zircon, tourmaline, altered mafic minerals, and opaque minerals.
			Wasatch Plateau, Utah			
29	Salina (McGookey, 1960).	Colton Formation; 530.	WP07–WP08	24 22 S., 1 E.	2 orange.	Poorly to moderately poorly sorted, fine- to coarse-grained. Quartz, dolomite, limestone, chert, and kaolinite in carbonate matrix. Accessory minerals: white mica, zircon, and opaque minerals; accessory minerals sparse.
			WP09–WP12	SE¼ 25 22 S., 1 E.	2 orange, 2 red.	Very poorly to poorly sorted, fine- to medium-grained. Quartz, fresh feldspars, dolomite, and limestone in carbonate matrix; patches of celestite matrix in WP09 and WP10. Accessory minerals: chert, zircon, tourmaline, garnet, white mica, sparse biotite, and opaque minerals.
30	Gunnison Plateau (Hardy and Zeller, 1953).	Colton Formation; 600.	WP01–WP06	12 16 S., 1 E.	3 orange, 2 yellow, 1 green.	Poorly to moderately well sorted, very fine to coarse-grained. Quartz, chert, and fresh to altered feldspars closely packed in clay matrix; WP06 has carbonate matrix. Accessory minerals: abundant altered biotite, garnet, zircon, tourmaline, epidote, chlorite, white mica, heulandite in WP03, analcime in WP05, and opaque minerals; accessory minerals abundant except in WP06.

TABLE 1. — *Sample localities, stratigraphic assignments, and petrographic descriptions of 216 samples of lower Eocene sandstone*—Continued

Locality No. (figs. 1, 5)	Area and reference	Stratigraphic unit; thickness (ft)	Field sample No.	Locality: Sec., T. and R.	Number of samples in specified color subset	Petrographic description
			Wasatch Range, Utah			
31	Woodruff (Stokes and Madsen, 1961).	Wasatch Formation; *0–1,000.	WM01–WM02	23 9 N., 5 E.	2 red.	Very poorly sorted, very fine grained to granular. Chert, quartz, and detrital limestone in calcite and hematite matrix. Accessory minerals: tourmaline, garnet, and zircon.
			WM03–WM04	18 9 N., 6 E.	2 red.	Poorly sorted, fine- to coarse-grained. Quartz and chert in hematite and kaolinite matrix. Accessory minerals: zircon, tourmaline, white mica, and opaque minerals (mostly in WM04).
			WM05–WM06	21 9 N., 6 E.	2 orange.	Poorly to moderately well sorted, very fine to coarse-grained. Quartz, chert, detrital limestone and dolomite in calcite matrix; calcite replaces some framework grains. Accessory minerals: zircon, tourmaline, white mica, and opaque minerals; biotite has been replaced by calcite (most accessory minerals in WM05).
32	Morgan (Mullens, 1971, p. D18).	Wasatch Formation; 5,000.	WM07–WM08	SE¼ 7 3 N., 3 E.	2 red.	Poorly sorted, coarse- to fine-grained. Quartz, chert, dolomite, limestone, kaolinite, and shale in calcite matrix. Accessory minerals: fresh to altered biotite, zircon, tourmaline, and opaque minerals; all mostly altered to calcite in WM07.
			WM09–WM12	S½ 9 3 N., 3 E.	4 red.	Very poorly to moderately well sorted, fine-grained to granular. Quartz, chert, dolomite, feldspars (except WM11), limestone, and shale in calcite and hematite matrix. Accessory minerals: zircon, tourmaline, altered biotite, and opaque minerals (very few accessory minerals in WM11–WM12).
			Washakie Basin, Wyo.			
33	Baggs (Bradley, 1964; Olson, 1959).	Wasatch Formation, main body; >500.	WK01–WK04	E½ 31 13 N., 91 W.	4 yellow.	Very poorly to moderately well sorted, fine- to coarse-grained. Quartz, generally fresh feldspars, chert, and shale in dirty clay matrix; gypsum matrix for WK01. Accessory minerals: fresh to altered green and brown biotite, white mica, zircon, garnet, tourmaline, chlorite, epidote, barite, vesuvianite, and opaque minerals.
		Wasatch Formation, Cathedral Bluffs Tongue; 1,250.	WK05–WK06	5 14 N., 92 W.	1 yellow, 1 orange.	Very poorly to poorly sorted, coarse-grained. Fresh to altered feldspars, quartz, chert, schist and quartzite in calcite and clay matrix. Accessory minerals: altered biotite, white mica, epidote, garnet, zircon, tourmaline, and opaque minerals.
34	Erickson–Kent Ranch (Bradley, 1964, p. A22; Roehler, 1970).	Wasatch Formation, main body; 1,700.	WK07–WK08	NE¼ 13 14 N., 102 W.	1 yellow, 1 orange.	Moderately well sorted, fine- to medium-grained. Quartz, altered feldspars, and clay (dolomite and limestone in WK08) closely packed in clay matrix with minor iron oxides. Accessory minerals: abundant biotite and white mica that are oriented parallel to the bedding, zircon, tourmaline, garnet, chloritoidlike minerals, and opaque minerals.
			WK09–WK10	SW¼ 19 14 N., 101 W.	2 yellow.	Moderately well sorted, fine-grained. Quartz, fresh to altered feldspars, detrital dolomite, and chert in brown-stained clay and calcite matrix. Accessory minerals: white mica, altered brown biotite, chlorite, abundant garnets, zircon, tourmaline, and opaque minerals.
		Wasatch Formation, Cathedral Bluffs Tongue; 850.	WK11–WK12	18 14 N., 99 W.	2 yellow.	Poorly sorted, fine-grained. Quartz, fresh to altered feldspars, and chert floating in calcite matrix. Micas occur along bedding planes, and biotite is in all stages of alteration. Accessory minerals: irregularly shaped garnets, tourmaline, chloritoidlike minerals, zircon, and opaque minerals.
			Wind River Basin, Wyo.			
35	Lost Cabin (Tourtelot, 1946; Keefer, 1965).	Wind River Formation, Lysite Member; 254.	WR07–WR10	SE¼ 15 39 N., 90 W.	3 orange, 1 yellow.	Very poorly to moderately well sorted, very fine to medium-grained. Quartz, silicified mudstone, dolomite, chert, and sandstone closely packed to floating in iron-rich carbonate matrix. Accessory minerals: biotite, white mica, glauconite, and zircon; framework grains contain a variety of accessory minerals.
		Wind River Formation, Lost Cabin Member, 173.	WR11–WR12	NE¼ 22 38 N., 89 W.	2 green.	Very poorly to poorly sorted, fine- to coarse-grained. Quartz, feldspars, chert, and limestone floating in iron-rich clay matrix. Accessory minerals: olive, bright-green, and bright-red biotite, white mica, glauconite, garnet, zircon, tourmaline, epidote, zoisite, and opaque minerals.
36	Wallace Creek (Rich, 1962).	Wind River Formation, upper coarse facies; 850.	WR13–WR14	NW¼ 21 32 N., 84 W.	2 yellow.	Very poorly sorted, granular to conglomeratic. Too friable for thin section.
		Wind River Formation, lower variegated facies; 275.	WR15–WR16	NE¼ 2 34 N., 87 W.	1 yellow, 1 orange.	Poorly sorted, coarse-grained to granular. WR16 too friable for thin section. WR15: Quartz and fresh to altered feldspars in composite grains closely packed in clay and biotite matrix. Accessory minerals: mostly zircon in composite grains.
		Wind River Formation, lower fine-grained facies; 500.	WR17–WR18	SW¼ 19 35 N., 86 W.	1 yellow, 1 orange.	Very poorly sorted, medium-grained to granular. WR17 too friable for thin section. WR18: Quartz and fresh to altered feldspars in composite grains in clay matrix. Accessory minerals: brown biotite, white mica, glauconite, chlorite, zircon, and opaque minerals.

The areas to be sampled were selected on the basis of published descriptions of a stratigraphic section in the areas or on the basis of personal knowledge of suitable outcrops. The location of the sampled areas are shown in figure 1, and the sample localities are listed in table 1. Because the Hoback basin is too small to warrant sampling at more than one place, the paired section was chosen from the westernmost end of the Wind River Basin; we thought that the geographic settings of the sequences in the two areas were sufficiently similar to negate the effects of deviating from the sample plan. Where possible, sandstone was sampled where a complete sequence of lower Eocene strata is exposed within a short horizontal distance. In some basins, roadside outcrops extending for several miles were sampled owing to the lack of better outcrops. Within the stratigraphic section in each area, three stratigraphic horizons were chosen at random. For example, the section might be divided into 50 or 100 equal parts and the three sample horizons picked from a table of random numbers from 1 to 100. If only a few sandstone beds were exposed within the section, the beds were numbered, and three beds were selected at random. After a sandstone bed near the randomly selected horizon was sampled, a paired sample was collected from the next higher or lower sandstone bed as determined by a toss of a coin. Each selected sandstone bed was divided into equal units 1–2 feet thick, and the exact sample site within the bed was chosen at random.

The samples averaged 5–10 pounds in weight, depending on the grain size of the sandstone. Weathering rinds, lichens, plant roots, concretions, iron-stained zones, large fossil fragments, and other obviously unrepresentative matter were looked for and were excluded where noticed. Every effort was made to sample fresh, unweathered outcrops. After we selected the sample horizon, we generally moved along the strike of the beds to find the least weathered location. If there were no unweathered outcrops, an alternate site was chosen. We also attempted to dig in beyond the most weathered part of the outcrop.

Where sandstone and mudstone beds alternate, picking the next higher or lower sandstone bed was no problem. In thick sandstone sequences having no obvious bedding, the paired sample was collected at least 20 feet above or below the first sample. Sets of cross strata were regarded as one bed. In conglomeratic sequences, samples were collected from the sandstone bed nearest the randomly selected locality or from the matrix of the conglomerate. In the field, recognition and distinction of sandstone from sandy varieties of other rock types generally was not difficult. Beds of sandy and conglomeratic mudstone were included in our definition of sandstone although their classification as such may be questionable. A more difficult distinction to make was between calcareous sandstone and sandy limestone. Although we attempted to exclude limestones, two samples collected from the Salina area of the Wasatch Plateau contain slightly more than 50 percent carbonate minerals.

METHODS OF ANALYSIS

One chip was removed from each sample for a thin section, and the rest was crushed and split for rapid rock analysis of major elements, direct-reader spectrometric analysis of minor elements, and X-ray-diffraction analysis of major minerals. Color was described from the ground and pelletized samples, using the color chart of Goddard and others (1948) for uniformity. Samples submitted for chemical and spectrometric analyses were arranged in a random sequence so that any potential analytical drift would be converted to random error. To estimate the precision of the analytical methods, 10 splits of one composite sample were included with the other samples without the analysts' knowledge. Results of the replicate analyses of the 10 hidden splits are shown in table 2. Good precision is indicated by the relatively small geometric deviations. The precision of analysis for the 216 samples is probably not this good, because the precision for each constituent varies somewhat with the amount of the constituent present. Rapid rock analyses were performed in the Washington laboratory of the U.S. Geological Survey

TABLE 2. — *Arithmetic mean, standard deviation, geometric mean, and geometric deviation of the analysis of 10 splits from one sample*

[Major-constituent analysis, rapid rock method, by Lowell Artis, S. D. Botts, G. W. Chloe, Paul Elmore, J. S. Glenn, James Kelsey, and H. Smith; minor-element analysis, direct-reader spectrometric method, by N. M. Conklin, R. G. Havens, and L. M. Lee]

	Arithmetic mean	Standard deviation	Geometric mean	Geometric deviation
Major constituents (in percent)				
SiO_2	54.83	0.38	54.81	1.01
Al_2O_3	11.20	.07	11.20	1.01
[1]Fe_2O_3	3.77	.05	3.77	1.02
MgO	4.28	.14	4.28	1.03
CaO	7.41	.68	7.38	1.09
Na_2O	1.40	.08	1.40	1.06
K_2O	3.84	.14	3.84	1.04
H_2O+	3.17	.46	3.14	1.15
TiO_2	.39	.03	.39	1.07
P_2O_5	.14	.04	.14	1.41
MnO	.08	.04	.07	2.2
CO_2	7.48	.21	7.48	1.03
Minor elements (in parts per million)				
B	41	16	38	1.6
Ba	2,350	412	2,318	1.8
Co	14	2	14	1.1
Cr	49	6	48	1.1
Cu	25	1	25	1.05
Ga	19	2	19	1.1
Ni	23	3	23	1.0
Pb	[2]13	[2]9	[2]10	[2]2.1
Sr	845	236	817	1.3
V	84	15	83	1.2
Zr	104	20	103	1.2

[1]Total iron as Fe_2O_3.
[2]Includes 5 samples reported to contain less than 20 ppm for which an arbitrary value of 5 ppm was assigned.

using the single solution wet chemical method described by Shapiro (1967). Direct-reader spectrometric analyses were performed in the Denver laboratory of the U.S. Geological Survey. A description of the direct-reader spectrometric method follows. The precision of the analytical results as it affects our interpretations of the geochemistry of lower Eocene fluvial sandstones is further discussed in the section on "Analysis of Variance."

DIRECT-READER SPECTROMETRIC ANALYSES

By RAYMOND G. HAVENS and ALFRED T. MYERS

Direct-reader spectrometric analysis of sandstone has evolved in the U.S. Geological Survey from a three-step semiquantitative method of analysis described by Myers, Havens, and Dunton (1961) and a later six-step semiquantitative method used with conventional spectrographs. When the direct-reading spectrometer is used, photoelectric recording and measurement of spectral line intensity replace the photographic recording of conventional spectrographs. The precision and accuracy of the direct-reader method as outlined here apply specifically to the sandstone samples in this report.

Synthetic standards are prepared from high-purity chemicals containing known concentrations of each element. By successive dilutions with a common matrix, a series of standards is obtained that covers a wide concentration range (Myers and others, 1961, p. 209–210, 225–228). Working curves covering the desired ranges of concentration for each element are established from these prepared standards.

Samples to be analyzed are ground to about 100 mesh or finer. A 10-mg (milligrams) portion of the sample is weighed and is thoroughly mixed with 20 mg of pure graphite powder. The sample-and-graphite mixture is then tamped into the cavity of a graphite electrode and is excited in a d-c arc. Table 3 gives the analytical conditions for the direct-reader spectrometric analysis of sandstone.

During the excitation period of the sample, radiation from the excited sample passes through the optics of the spectrometer and strikes the photomultiplier tubes which convert the radiation energy into electric current. By the end of the exposure period, the current from a photomultiplier has charged a capacitor to a specific voltage which is proportional to the integrated intensity of the associated spectral line and, therefore, to the concentration of the particular element in the sample.

The spectral lines used for the elements reported are shown in table 4, along with the width of the exit slits and the concentration range covered for each element. Table 2 indicates the precision obtained from 10 hidden splits that were submitted at the time of analysis. In table 5 the results obtained on the U.S. Geological Survey standard rock samples G–1 and W–1 are compared with the recommended values (Fleischer, 1969) for the standard rocks.

TABLE 3.—*Analytical conditions for the direct-reader spectrometric analysis of sandstone*

Spectrometer	Consolidated Electrodynamics Corp. 3-meter, type 22–101.
Grating	21,000 lines per inch.
Dispersion	3.9i A/mm.
Spectral region	2100–5200 A.
Slit width (entrance)	25μ.
Excitation source	d-c arc.
Voltage (open circuit)	350 v.
Current (short circuit)	16 amps.
Analytical gap	5 mm.
Exposure at 6 amp	6 sec.
Exposure at 16 amp	114 sec.
Exposure total	120 sec.
Sample electrodes	Ultra Carbon Corp., type 3170–U2.
Counter electrodes	Made from Ultra Carbon Corp. high-purity ¼-inch graphite rod.
Graphite powder	Ultra Carbon Corp. UCP–2, conducting.

TABLE 4. — *Spectral lines used for the elements reported and the concentration ranges covered*

Element	Spectral line (angstroms)	Width of exit slit (microns)	Concentration range covered (parts per million)
B	2,496.78	50	30– 1,000
Ba	4,554.03	50	10–10,000
Co	3,453.50	100	8– 1,000
Cr	4,274.80	100	5– 1,000
Cu	3,247.54	100	1– 1,000
Ga	2,943.64	50	10– 1,000
Ni	3,414.76	50	7– 1,000
Pb	2,833.06	50	20– 1,000
Sr	4,607.33	50	10– 5,000
V	4,379.24	100	10– 1,000
Zr	3,279.26	100	20– 1,000

TABLE 5.—*Comparison of direct-reader spectrometric analyses with recommended values*

[All values are in parts per million]

Element	Sample G–1		Sample W–1	
	Direct reader	Recommended[1]	Direct reader	Recommended[1]
B	<30	1.5	<30	15
Ba	1,100	1,200	200	180
Co	<8	2.4	42	50
Cr	16	22	150	120
Cu	15	13	100	110
Ga	22	18	24	16
Ni	<7	1–2	76	78
Pb	43	49	<20	8
Sr	330	250	200	180
V	21	16	270	240
Zr	180	210	100	100

[1]All values, except those for B, are from Fleischer (1969, table 5), who listed recommended values for most elements based on determinations by various methods from different laboratories. For B, the above figures are listed as suggested magnitudes.

X-RAY DIFFRACTION ANALYSES

The relative mineral composition of samples was determined by X-ray diffraction analysis of whole rock splits. These data are expressed as inches of deflection of the X-ray diffractometer recording needle (peak heights) above background. This method does not determine absolute quantities of minerals detected but does permit comparison of approximate mineral contents between samples. Hand-ground and pelletized samples were scanned from 2° to 60° 2θ at a rate of 2° per minute on a Norelco X-ray diffractometer using nickel-filtered CuK alpha radiation generated at 48 kilovolts and 20 milliamperes and a geiger-counter. Reflection intensities, or peak heights, were measured above background, using the principal peak for each mineral

as follows: Quartz, 4.26 A; potassium feldspar, 3.24 A; plagioclase, 3.19 A; calcite, 3.04 A; dolomite, 2.89 A; laumontite, 9.15 A; clinoptilolite, 9.00 A; and analcime, 5.61 A. The clay minerals having principal peaks between 11 and 15 A were grouped under the name "mixed-layer clays," abbreviated MLC, and probably include montmorillonite, chlorite, and mixtures like illite-montmorillonite. Minerals having a principal peak at 10 A were grouped under the term "mica" but may include some illite and mixed-layer clays. The 7–A clays were grouped under the term "kaolin." Inasmuch as detailed analyses would be needed to identify positively any specific clay mineral, quotation marks are used in referring to clay species.

Increased iron content can affect the peak heights by raising the background of the diffractogram. However, in the lower Eocene sandstone samples the iron content generally was not large enough to seriously affect the comparisons. Chert, which was measured with quartz, makes the quartz peak slightly broader and lower than it would be if quartz alone were present. These are semiquantitative measurements, which are sufficient for comparative purposes but which have neither the accuracy nor the precision for quantitative data. Because different minerals reflect the X-rays at different intensities, the data as they are presented here should be used only to compare amounts of one mineral in different samples, not amounts of different minerals in one sample. The limits of detection range from about 2 to 5 percent depending on the composition of the sample and on the crystallography of the specific mineral. Though semiquantitative, the data from the X-ray analyses are useful for a classification of the sandstones included in this study (fig. 3).

PETROLOGY AND MINERALOGY

All but the most friable samples of sandstone were examined in thin section for textural relations and for accessory minerals not detected by X-ray diffraction analysis. Heavy-mineral and clay-mineral separates were also made on selected samples, and mineral identifications, where needed to supplement the thin-section studies, were made by X-ray or optical methods. The texture and mineralogy of the samples are described in table 1.

MINERAL COMPOSITION AND CLASSIFICATION OF SAMPLES

Quartz and varying proportions of chert, potassium feldspar, plagioclase, mica, calcite, and dolomite are the principal framework minerals in most samples. In most samples they occur as separate mineral grains; in some they are in composite grains such as granite, schist, shale, limestone, dolomite, and sandstone fragments. To classify the lower Eocene sandstone samples, a triangular diagram was constructed,

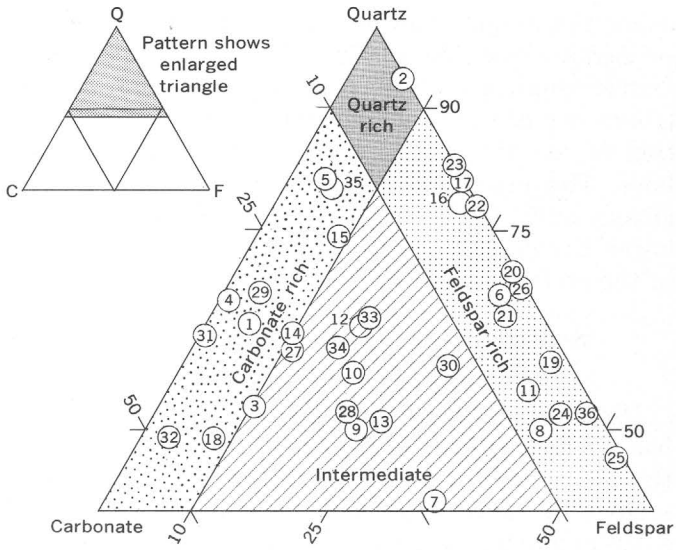

FIGURE 3. — Average composition of lower Eocene sandstone in 36 areas in the Rocky Mountain region. Mineral data normalized from X-ray diffraction analyses for quartz, feldspars, and carbonate minerals. Minor amounts of zeolites were included with the feldspars for some areas. Clay minerals, mica, and other accessory minerals were not included. Some areas contain minor amounts of feldspars and carbonates that are not represented in this figure because they fall below the limit of detection by the X-ray method. Numbers within each circle are keyed to the areas listed in table 1 and are shown in figure 1.

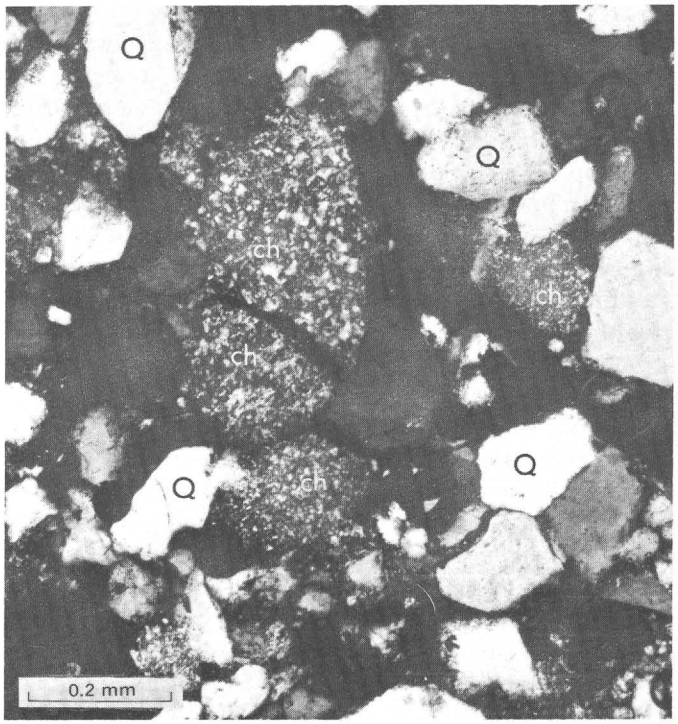

FIGURE 4. — Photomicrograph of quartz-chert sandstone from the Willwood Formation, Hillberry Rim area, Bighorn Basin, Wyo., showing chert grains (ch), which are readily distinguished by their mottled appearance under crossed polars, and clear quartz grains (Q). Crossed polars; sample BH03.

having quartz, feldspar, and carbonate as end members (fig. 3). The mean content, in percent, of the end members in each set of six samples was roughly estimated from the X-ray diffraction analyses, and

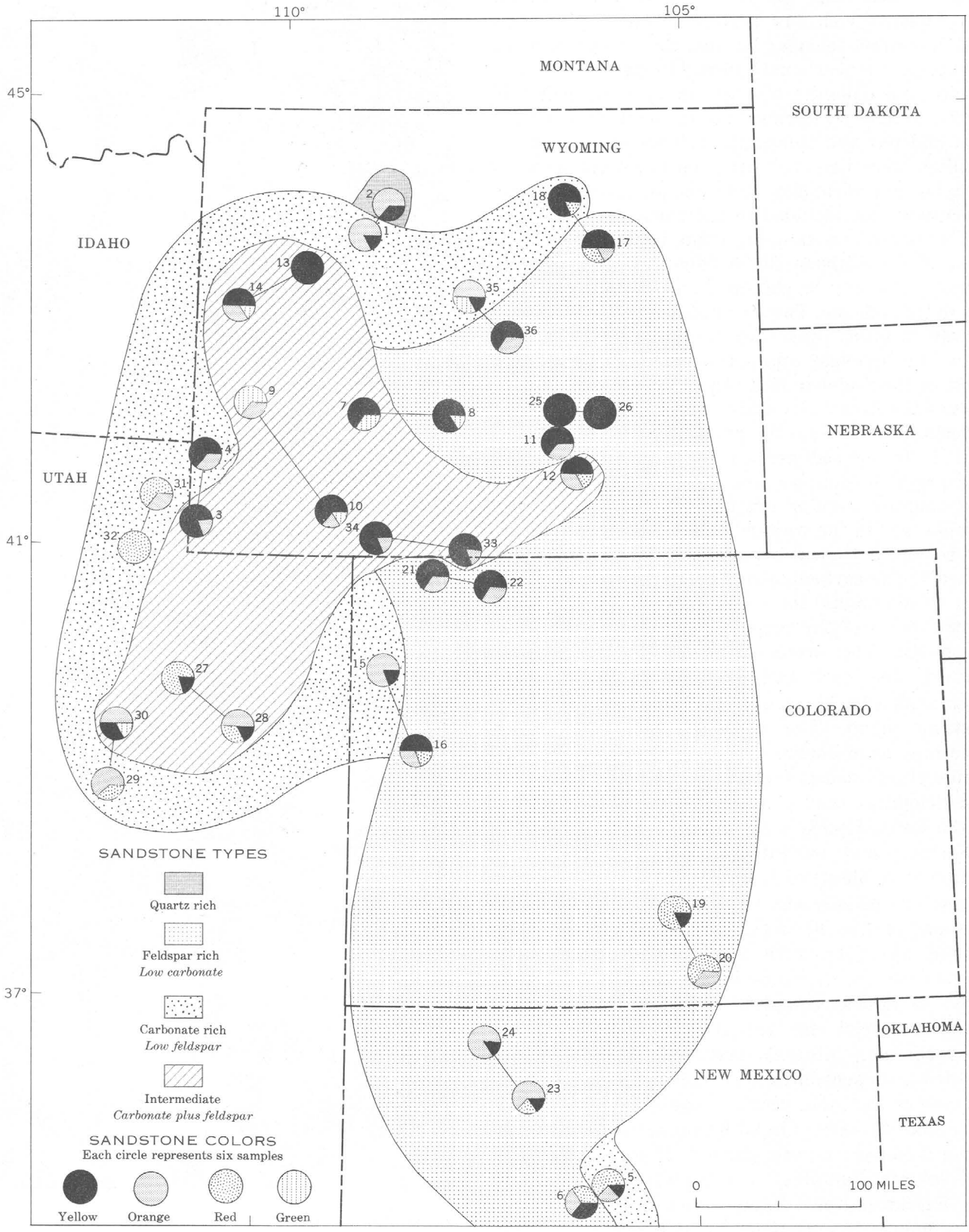

FIGURE 5. — Distribution of lower Eocene sandstone types, and colors of the sandstone in powdered samples in 36 areas in the Rocky Mountain region.

sample sets were plotted on the diagram. The diagram was then divided into four parts: (1) quartz rich (greater than 90 percent quartz and chert), (2) feldspar rich (10 percent or more plagioclase and potassium feldspar but less than 10 percent carbonates), (3) carbonate rich (10 percent or more calcite and dolomite but less than 10 percent feldspar), and (4) intermediate (greater than 10 percent feldspar and greater than 10 percent carbonate). Zeolites were included with the feldspars in a few samples, but mica, clay minerals, and accessory minerals were not included in the calculations.

The sandstone samples from the Hillberry Rim area of the Bighorn Basin (figs. 3–5) are the only samples that can be classified as quartz rich according to this scheme. These samples have a clay matrix, mostly "kaolin," and they contain about 5 percent potassium feldspar and a few grains of plagioclase. Most of the feldspar-rich sandstone is in the eastern part of the Rocky Mountain region (fig. 5). This fact reflects the dominantly crystalline source terrane (fig. 1) of the sediments in basins to the east. The feldspar-rich samples are generally poorly sorted and contain angular grains (fig. 6). Intermediate samples are in the western and west-central parts of the region. A typical intermediate sample is shown in figure 7. The carbonate-rich samples occur in a band that wraps around the northern, western, and south-central parts of the region and in the Cerrillos area in the Gallisteo basin. In most thin sections examined, the carbonate minerals occur in lithic fragments (fig. 8) as well as in the matrix as a cementing agent. The carbonate-rich samples are generally near source terranes composed of older sedimentary rocks, including Paleozoic limestones and dolomites that probably contributed carbonate to the lower Eocene sandstones.

Etching and partial dissolution of framework grains were observed in many thin sections. Quartz grains are usually etched in samples having a calcite matrix (fig. 9). Feldspar grains are commonly altered along fracture and cleavage planes. The plagioclase grains range in appearance from unaltered to almost completely altered, regardless of matrix material (fig. 10). Sericite and clay are the most common minerals replacing plagioclase, but zeolites and carbonates also replace feldspars.

Some of the more common nonopaque heavy minerals that were noted in both thin sections and heavy-mineral separates are garnet, zircon, tourmaline, and epidote. Samples from the Firehole Basin and the Erickson–Kent Ranch areas contain garnets large enough to appear out of hydraulic equilibrium with the quartz and other framework grains. Their large size suggests unusual conditions of deposition,

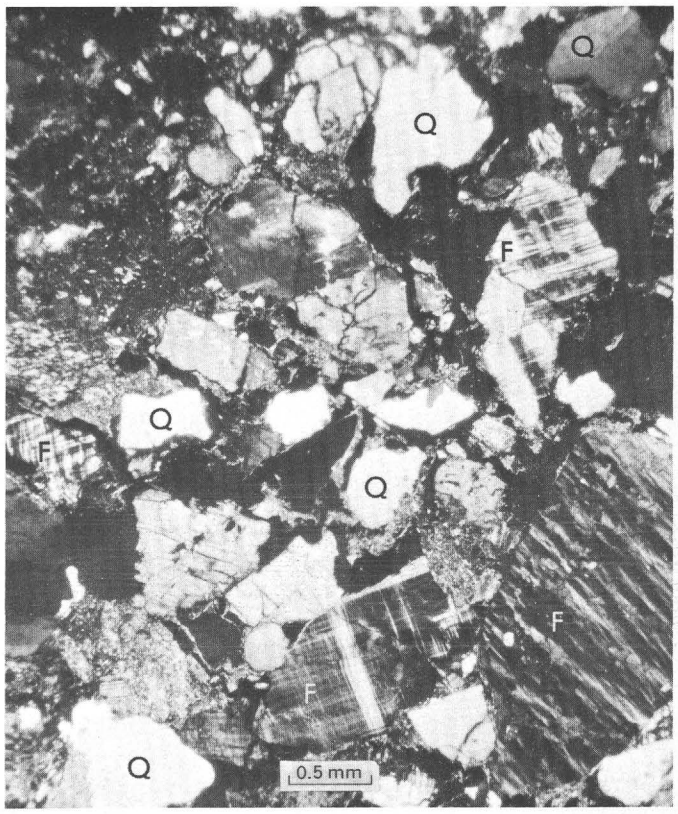

FIGURE 6. — Photomicrograph of arkosic sandstone from the Wind River Formation, Wallace Creek area, Wind River Basin, Wyo., showing poorly sorted, closely packed, angular grains of quartz (Q) and feldspar (F) in a clay matrix. Crossed polars; sample WR15.

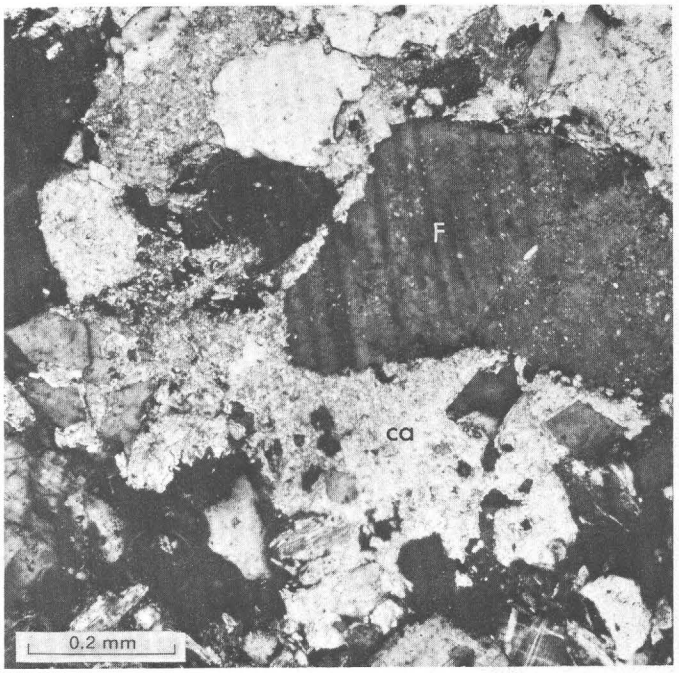

FIGURE 7. — Photomicrograph of an intermediate sandstone, Wasatch Formation, Oregon Buttes area, Great Divide Basin, Wyo., showing abundant feldspar (F) and calcite (ca). Crossed polars; sample GD05.

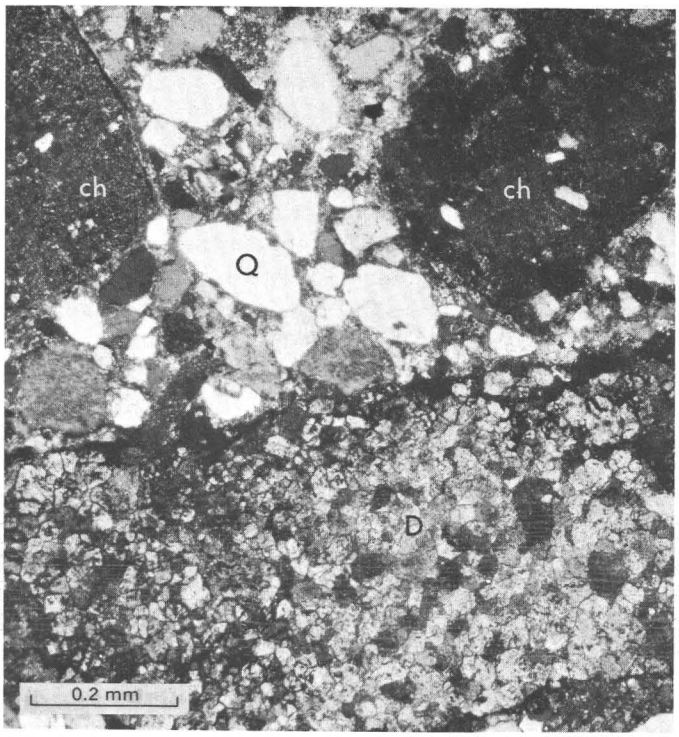

FIGURE 8. — Photomicrograph of lithic sandstone from the Wind River Formation, Lost Cabin area, Wind River Basin, Wyo., showing very poorly sorted fragments of dolomite (D), chert (ch), and quartz (Q) in a matrix of iron-stained carbonate. Crossed polars; sample WR09.

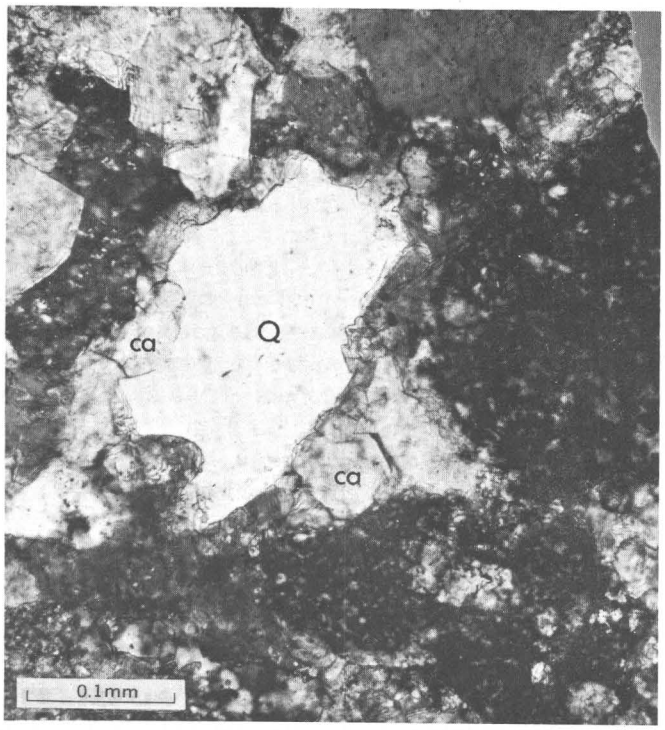

FIGURE 9. — Photomicrograph of etched quartz grain from the Wasatch Formation, Woodruff area, Wasatch Range, Utah. Outline of original quartz grain (Q) is no longer discernible; the present ragged outline is the result of replacement by calcite (ca). Crossed polars; sample WM06.

FIGURE 10. — Photomicrograph of altered feldspar grain from the Hanna Formation, Difficulty area, northern Hanna basin, Wyoming. A large plagioclase grain (P) has been partly altered to sericitic mica, which forms the mosaic of minute light-colored crystals. The original plagioclase twinning is faintly visible in the upper part of the grain and in the dark unaltered region surrounding an embayment by calcite (ca). Crossed polars; sample HN06.

although most of these samples are derived from obvious channel sandstones. In the thin sections, the nonopaque minerals ranged in amounts from none (Hagen area) to as much as 5 percent (Hoback basin). Hornblende and augite were rarely observed, even in the heavy-mineral separates. They seem unusually sparse in these areas relative to their abundance in modern stream and terrace deposits derived from some of the same source areas (Denson, 1969, p. C29).

CEMENT AND MATRIX

Cementing and matrix minerals compose 5–20 percent of the total rock in most lower Eocene sandstone samples and may comprise as much as 50 percent of the rock in a few samples. With one or two exceptions, none of the sandstone examined in thin sections could be described as clean or well sorted (table 1). In many samples the wide range in the size of framework grains obscured any clear distinction between framework grains and matrix or cementing minerals.

A wide variety of matrix minerals was found in the lower Eocene sandstones. Clay minerals include abundant "kaolin" in the Enos Creek, Carbon basin, Cerrillos, Hoback basin, Battlement Mesa, Horse Creek–Crazy Woman Creek, Soldier Summit, and

Morgan areas (1, 12, 5, 14, 16, 18, 27, and 32 in fig. 1). "Montmorillonite," "chlorite," or "mixed-layer clays" are abundant in the Hagen, Battlement Mesa, Huerfano Park, Little Snake River, and Soldier Summit areas (6, 16, 19, 21, and 27 in fig. 1). Detrital clay minerals were difficult to distinguish from authigenic clay minerals, although some clay could be recognized as authigenic where a single clay mineral species forms a uniformly textured matrix, filling cavities throughout the rock (fig. 11), or where the clay mineral forms oriented coatings on framework grains (fig. 12) or partly replaces framework grains.

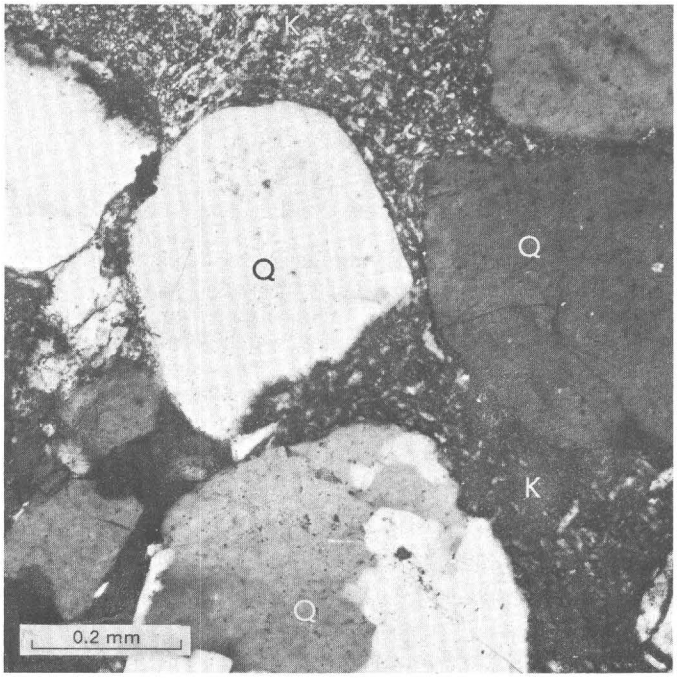

FIGURE 11. — Photomicrograph of sandstone from the Willwood Formation, Enos Creek area, west flank of the Bighorn Basin, Wyoming, showing a uniformly textured clay cement. Grains of quartz (Q) are cemented by "kaolin" (K) that is thought to be authigenic because of its uniform texture throughout the thin section. Crossed polars; sample BH07.

Carbonate cement is common in many samples—especially those from the Enos Creek, Evanston, Fossil, Horse Creek–Crazy Woman Creek, Woodruff, Morgan, and Salina areas (1, 3, 4, 18, 31, 32, and 29 in fig. 1). Dolomite or ankerite is also abundant in the Patmos Head, Soldier Summit, and Salina areas (28, 27, and 29 in fig. 1). Zeolites are abundant in the West Spanish Peak and Patmos Head areas (20 and 28 in fig. 1) and were also found in the Firehole Basin, La Barge, Pine Ridge–Pumpkin Buttes, and Gunnison Plateau areas (10, 9, 17, and 30 in fig. 1). Gypsum and celestite were found in the Baggs and Salina areas, respectively (33 and 29 in fig. 1).

Red, orange, and yellow iron oxides form stains and cements in most of the samples. Many of these oxides are the product of surficial weathering, but sampling below the zone of oxidation was impractical. No certain distinction exists between recent weathering and postdepositional or diagenetic effects. However, reds generally indicate the presence of hematite, or some incompletely crystalline variety of hematite, and are more likely to be the result of diagenetic processes. Oranges and yellows indicate the presence of goethite, limonite, and similar amorphous ferric hydrates and are more likely to be the result of weathering processes. (See Walker, 1967, for a more extended discussion of the relation of iron oxide mineralogy to color and geologic processes.) Orange and yellow stains in deep roadcuts and mine cuts indicate that the zone of oxidation may extend several hundred feet below the surface locally, depending on rock permeability, chemical reactivity, and ground-water level.

DIAGENESIS AND METAMORPHISM

Except for weathering, all chemical, mineralogical, and textural changes that take place in a buried sediment under near-surface conditions of relatively low temperature and pressure are generally regarded as diagenetic (Taylor, 1964). If such authigenic cementing materials as clay, carbonate, sulfate, zeolite, and red iron oxide minerals are regarded as diagenetic, then nearly all samples of lower Eocene sandstones include evidence of diagenesis. Further evidence of diagenesis is the corrosion, etching, or dissolution of framework grains that is seen in many samples and the presence of several less common authigenic minerals in some samples, including epidote and glauconite (Vine and Tourtelot, 1970a).

The distinction between diagenetic and metamorphic changes in a sediment is an arbitrary one. However, minerals that are indicative of elevated temperatures and pressures are generally used to classify a rock as metamorphic. One such mineral, laumontite, a calcium zeolite, has been reported (Vine, 1969) in several samples from the Spanish Peaks area of Colorado (fig. 13). Laumontite has been described (Coombs and others, 1959) as characteristic of the zeolite facies of metamorphism that is transitional between diagenesis and conventional metamorphism. Laumontite can also be regarded as characteristic of low-grade hydrothermal metamorphism resulting from elevated temperature without deep burial and accompanying high pressure (Sharp, 1970; D. S. Coombs, oral commun., 1970). Alteration of sandstone in the Spanish Peaks area probably occurred when geothermal gradients were increased by intrusion of the East Spanish Peaks stock and

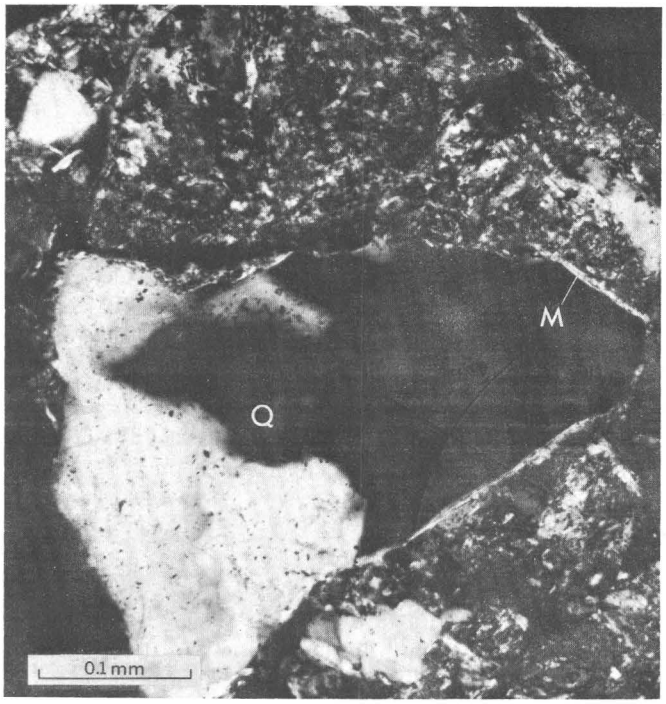

FIGURE 12. — Photomicrograph of sandstone from the Wasatch Formation, Elkhead Mountains area, Sand Wash Basin, Colorado, showing an authigenic montmorillonite matrix. An angular grain of quartz (Q) is surrounded by a thin bright rim of strongly birefringent montmorillonite (M) that also forms most of the cement between the framework grains. Crossed polars; sample SW08.

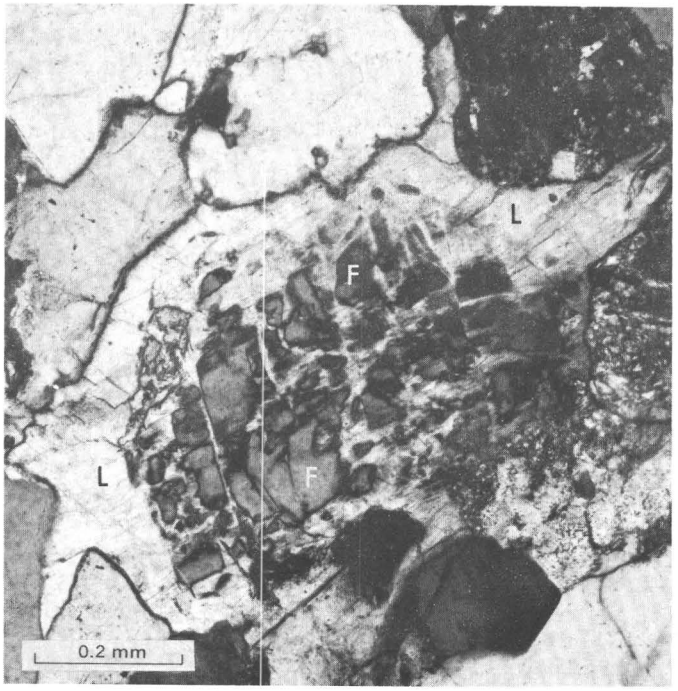

FIGURE 13. — Photomicrograph of laumontite-cemented sandstone from the Cuchara Formation, Spanish Peaks area, Raton basin, Colorado. Laumontite (L) forms the cement and partly replaces a feldspar grain (F). Crossed polars; sample LE 259B.

the numerous dikes associated with the West Spanish Peaks volcanic vent.

Compound grains of epidote and feldspar (fig. 14) are fairly common in some thin sections (table 1). Because epidote grains are brittle and feldspar has good cleavage, it would be highly fortuitous for compound grains to survive abrasion during transport. We have, therefore, regarded these occurrences as evidence for the authigenic origin of the epidote. As there is no evidence other than the authigenic epidote to suggest elevated temperature or metamorphism, we conclude that epidote is a normal diagenetic mineral in some of these samples.

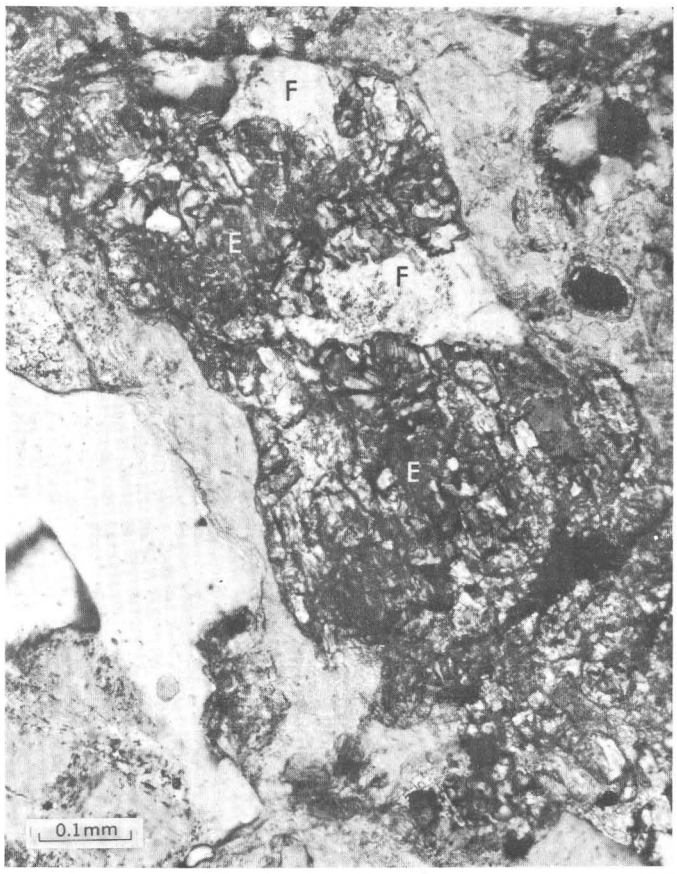

FIGURE 14. — Photomicrograph of arkosic sandstone from the Wasatch Formation, Oregon Buttes area, Great Divide Basin, Wyoming, showing feldspar grain (F) partly replaced by epidote (E). Crossed polars; sample GD06.

Some aspects of the geochemical history of the lower Eocene sandstones are revealed by the type and degree of diagenetic alteration. With the possible exception of authigenic "kaolin," most of the authigenic minerals and changes observed suggest alteration by alkaline pore waters. The etching and dissolution of silicate minerals, the replacement of framework grains, and the filling of voids by calcite, dolomite, analcime, clinoptilolite, laumontite, or "montmorillonite" are regarded as an indication of

diagenesis by alkaline solutions, generally alkaline carbonate solutions (Hay, 1966, p. 67, 70, 77, 84; Sheppard and Gude, 1969, p. 26–29; Muffler and White, 1969, p. 177–179; Hawkins and Whetten, 1969).

CHEMICAL COMPOSITION OF SANDSTONES

STATISTICAL METHODS

Summary statistics were compiled for the element and major mineral composition of the lower Eocene sandstones from the chemical, spectrometric, and X-ray diffraction analyses. These compilations made use of statistical programs for geochemical studies available through the computer facilities of the U.S. Geological Survey. Arithmetic and geometric means were calculated for each of nine major minerals or mineral groups, 16 minor elements, and 16 major elements or oxides of the elements for 216 samples (table 7). Because many of the computations involve logarithmic transformation, arbitrary real values were assigned to all determinations reported as "greater than," "less than," or "not detected" by the analysts. The substitutions used for indeterminate values are listed in table 6. The calculations, in general, are not particularly sensitive to a small number of substitutions. The elements B, Co, La, Pb, and Y were omitted from those statistical calculations that are most sensitive to a large number of substitutions. In table 7, mean values are not listed for areas where an element was below the limit of detection for most of the samples. For such elements the mean values for the total set of 216 samples must be viewed as a rough estimate. The summary values listed in table 7 for U and Th are based on a total of only 86 samples, and many of the values listed under individual areas represent single samples. Moreover, these two elements were not included in any of the subsequent computations. Mean values were calculated for "mixed layer clays" (MLC) and dolomite even though more than 50 percent of the values were indeterminate. The results for these minerals are less trustworthy than those for the other minerals. For indeterminate mineral values, a very low replacement value, approaching zero, was used in computing statistical measures because, unlike elements, certain mineral species may be totally absent in some rocks.

TABLE 6. — *Limits of detection and values used to replace indeterminate analyses*

	Number of indeterminate values	Minimum value detected	Replacement value
Major constituents (in percent)			
Fe_2O_3[1]	11	0.06	0.05
MgO	4	.07	.06
CaO	1	.09	.08
Na_2O	19	.03	.02
H_2O-	1	.02	.01
TiO_2	3	.03	.02
P_2O_5	29	.02	.01
MnO	18	.02	.01
CO_2	57	.05	.03
Total C	41	.02	.005
Minor elements (in parts per million)			
Mn	3	7	6
B	176	30	10
Ba	1	50	40
Co	119	8	2
Cr	49	5	3
La	196	51	10
Ni	68	7	3.5
Pb	158	20	5
Sr	9	20	19 ([2]34,000)
V	29	10	8
Y	131	20	5
Ga	98	10	5
Minerals (in inches of deflection)			
"MLC"	140	0.01	0.001
"Mica"	57	.1	.001
"Kaolin"	62	.1	.001
Potassium feldspar	29	.1	.001
Plagioclase	59	.1	.001
Calcite	106	.1	.001
Dolomite	124	.1	.001
Zeolite	199	.1	.001

[1]Total iron as Fe_2O_3.
[2]Replacement value, based on rapid rock analysis, for one indeterminate value reported as "greater than 5,000 ppm."

MEANS

In preparing a statistical summary of chemical and mineralogical data, one must choose measures of central tendency and dispersion. In a preliminary summary of this investigation (Vine and Tourtelot, 1970a), we reported the arithmetic means and standard deviations of the constituents detected for 228 samples and for each set of 12 samples from 19 different basins of deposition. In the present report the 12 samples collected from the Bearpaw Mountains in Montana have been excluded, and only the data on the remaining 18 basins of deposition are summarized (table 7) and used for deriving other statistical measures. In the earlier report, the arithmetic mean was tabulated for each set of 12 samples from each basin. In the present report the geometric mean for each set of six samples from each area sampled has been tabulated. As can be seen in table 7, values for areas within a single basin vary considerably.

Many elements in nature tend to show lognormal distributions (Ahrens, 1954), and thus logarithmic transformations are commonly used in statistical studies of geochemical data. In the total set of 216 samples of lower Eocene sandstones, most constituents approach lognormal distribution, but SiO_2, Al_2O_3, K_2O, and TiO_2 more nearly approach normal distribution than lognormal. Most of the minor elements show a lognormal distribution with a skewness of less than 0.75 when measured as g_1 (Snedecor and Cochran, 1967, p. 86). Exceptions consist of B, La, and Pb, which have truncated distributions owing to the large number of indeterminate values reported. The major minerals also approach lognormal distribution except for potassium feldspar, which has a more normal distribution pattern, and zeolite, which shows extreme positive skewness. Calcite has an almost perfectly symmetrical lognormal distribution. All the minerals show positive skewness

TABLE 7. — *Distribution of constituents in 216 samples of lower Eocene sandstone and in 36 areas and four color subsets of the samples*

[Data for SiO_2 through CO_2 from rapid rock analyses by Lowell Artis, S. D. Botts, G. W. Chloe, P. L. D. Elmore, J. S. Glenn, James Kelsey, and H. Smith; for total C, from induction-furnace analyses by I. C. Frost, E. J. Rowe, G. D. Shipley, and Winona Wright; for Fe through Ga, from direct-reader spectrometric analyses by N. M. Conklin, R. G. Havens, and L. M. Lee; for U and Th, from gamma-ray spectrometer analyses by C. A. Bush and C. M. Bunker; for minerals, from X-ray diffraction analyses by the authors. Leaders (.....) indicate insufficient data or not analyzed.]

	Major constituents in percent															
	SiO_2	Al_2O_3	Fe_2O_3	MgO	CaO	Na_2O	K_2O	H_2O+	H_2O-	TiO_2	P_2O_5	MnO	CO_2	Total C	Fe	Ti
Geometric means and geometric deviations of analyses of 216 lower Eocene sandstone samples																
Geometric mean	72.90	6.59	1.15	0.55	2.36	0.51	1.41	1.35	0.32	0.20	0.050	0.056	0.71	0.23	0.76	0.091
Geometric deviation	1.19	1.92	2.14	3.00	4.34	4.56	2.34	1.59	2.89	1.94	2.55	2.06	12.56	11.55	1.87	1.74
Geometric mean × GD	86.75	12.65	2.46	1.65	10.24	2.33	3.30	2.15	.92	.39	.128	.115	8.92	2.66	1.42	.158
Geometric mean ÷ GD	61.26	3.43	.54	.18	.54	.11	.60	.85	.11	.10	.020	.027	.057	.020	.41	.052
Geometric means of analyses of six samples from each of 36 areas																
Locality (area in fig. 1)																
Bighorn Basin, Wyo.:																
Enos Creek (1)	65.02	6.33	2.78	1.10	6.74	0.11	0.99	1.84	0.19	0.20	0.066	0.068	4.22	2.04	0.93	0.072
Hillberry Rim (2)	86.88	4.30	1.76	.22	.47	.04	.72	1.70	.22	.25	.022	.027	.12	.08	1.02	.11
Fossil basin, Wyo.:																
Evanston (3)	63.07	3.36	1.09	1.34	11.51	.06	.86	1.15	.12	.24	.18	.054	9.87	1.92	.57	.080
Fossil (4)	75.62	2.85	.59	1.15	8.21	.16	.38	1.04	.14	.09	.18	.071	7.96	1.89	.41	.045
Galisteo basin, N. Mex.:																
Cerrillos (5)	83.62	3.79	.50	.15	2.29	.13	.68	1.17	.15	.11	.016	.055	.83	.40	.38	.059
Hagen (6)	74.69	10.47	1.60	.59	1.29	1.43	2.08	1.99	1.85	.32	.042	.074	.12	.05	.86	.11
Great Divide Basin, Wyo.:																
Oregon Buttes (7)	67.76	9.89	1.73	.78	4.47	1.69	2.02	1.09	.45	.24	.059	.12	1.22	.25	1.55	.12
Crooks Gap–Wamsutter (8)	75.56	11.44	1.03	.27	.93	1.29	3.39	1.67	.48	.11	.029	.029	.30	.13	.81	.067
Green River Basin, Wyo.:																
La Barge (9)	65.93	9.54	1.91	1.32	5.19	.74	2.08	1.88	.25	.32	.10	.071	2.69	.53	1.34	.15
Firehole Basin (10)	71.59	7.72	2.10	1.23	4.85	.81	1.68	1.10	.20	.31	.11	.082	4.08	1.18	1.35	.15
Hanna basin, Wyo.:																
Difficulty (11)	79.09	8.77	.73	.13	.51	1.48	3.25	.89	.16	.12	.017	.053	.12	.04	.58	.057
Carbon basin (12)	68.49	6.97	1.48	.76	3.56	.26	1.10	1.72	.16	.25	.033	.038	2.93	.80	.76	.11
Hoback-western Wind River Basins, Wyo.:																
Dubois (13)	65.47	8.54	1.22	2.24	6.30	1.23	1.75	1.42	1.51	.23	.11	.045	3.17	1.81	.76	.080
Hoback basin (14)	68.52	6.26	1.69	1.29	6.24	.48	1.08	1.63	.67	.25	.072	.087	3.61	1.04	.83	.098
Piceance Creek basin, Colo.:																
Rangely (15)	79.49	4.37	.78	.76	3.35	.45	1.27	1.06	.13	.19	.054	.048	2.42	.57	.52	.080
Battlement Mesa (16)	82.96	7.62	.76	.30	.62	.91	1.27	1.77	.48	.34	.026	.057	.15	.052	.54	.14
Powder River Basin, Wyo.:																
Pine Ridge–Pumpkin Buttes (17)	87.92	4.62	.62	.24	.31	.33	1.28	1.12	.29	.22	.027	.028	.....	.017	.45	.099
Horse Creek–Crazy Woman Creek (18)	46.46	7.74	2.15	1.01	14.62	.27	1.17	1.81	.47	.28	.14	.095	6.59	2.83	.87	.087
Raton basin, Colo.:																
Huerfano Park (19)	75.68	11.52	1.42	.27	1.04	1.05	3.51	1.96	.68	.23	.040	.061	.21	.033	1.07	.097
West Spanish Peak (20)	77.60	10.71	2.01	.66	1.65	1.61	1.04	1.88	.43	.25	.045	.055	.....	.016	1.38	.11
Sand Wash basin, Colo.:																
Little Snake River (21)	78.14	9.63	1.19	.42	1.17	1.25	3.20	1.10	.72	.18	.074	.033	.23	.034	.77	.089
Elkhead Mountains (22)	82.21	8.00	1.32	.22	.38	.29	1.93	1.55	1.04	.17	.023	.041	.055	.039	.92	.091
San Juan Basin, N. Mex.:																
Cuba (23)	86.81	5.78	.62	.18	.69	.42	1.57	1.07	.18	.23	.020	.050	.04	.053	.51	.082
Gobernador (24)	76.29	10.47	1.59	.37	1.85	3.15	2.27	.90	.19	.26	.025	.065	.41	.16	1.33	.14
Shirley Basin, Wyo.:																
Bates Hole (25)	76.02	12.85	.83	.26	1.00	2.42	3.62	1.23	.49	.17	.030	.037	.04	.017	.80	.073
Chalk Hills (26)	80.52	9.79	1.07	.17	.35	.46	4.13	1.56	.80	.18	.025	.034	.04	.007	.64	.079
Uinta Basin, Utah:																
Soldier Summit (27)	66.21	7.78	1.72	2.11	8.27	.71	.72	2.12	.47	.32	.076	.10	8.14	2.33	.77	.11
Patmos Head (28)	63.40	10.39	2.55	1.84	4.43	2.40	1.99	1.76	.46	.41	.084	.094	3.76	1.34	1.69	.19
Wasatch Plateau, Utah:																
Salina (29)	70.91	1.83	.34	1.48	10.03	.14	.52	1.03	.24	.14	.049	.071	8.99	2.27	.26	.051
Gunnison Plateau (30)	75.85	6.73	1.24	.68	2.51	1.06	1.56	.97	.26	.30	.061	.046	.67	.079	.98	.16
Wasatch Range, Utah:																
Woodruff (31)	68.26	1.74	.40	.14	4.64	.06	.19	.87	.09	.16	.084	.068	2.21	.46	.32	.051
Morgan (32)	57.34	2.48	.85	1.04	14.71	.05	.60	.91	.05	.10	.091	.084	12.51	3.34	.41	.043
Washakie Basin, Wyo.:																
Baggs (33)	74.19	7.03	1.20	.40	2.27	.76	1.35	1.61	.73	.21	.047	.060	.54	.17	.75	.10
Erickson–Kent Ranch (34)	70.73	7.58	1.29	.70	4.84	1.27	1.89	1.07	.13	.16	.075	.072	2.38	.85	.88	.12
Wind River Basin, Wyo.:																
Lost Cabin (35)	77.82	4.67	1.57	1.41	3.45	.17	1.10	1.54	.38	.23	.13	.052	2.46	.91	.95	.11
Wallace Creek (36)	77.83	11.82	.91	.24	.53	2.48	3.87	1.18	.36	.09	.015	.030	.033	.011	.81	.075
Geometric means of analyses of samples from four subsets grouped on the basis of color																
40 red sandstones	72.68	5.20	0.97	0.54	2.69	0.36	0.94	1.39	0.26	0.22	0.050	0.066	0.85	0.22	0.63	0.090
67 orange sandstones	74.22	5.58	1.17	.49	2.73	.38	1.21	1.26	.23	.17	.048	.056	.93	.34	.77	.082
98 yellow sandstones	72.63	7.67	1.13	.54	1.96	.64	1.76	1.34	.40	.21	.048	.050	.51	.17	.73	.091
11 green sandstones	68.24	11.19	2.37	1.37	3.19	1.43	2.23	1.98	.57	.38	.091	.076	1.39	.44	1.77	.19

	Minor elements, in parts per million															
	Mn	B	Ba	Co	Cr	Cu	La	Ni	Pb	Sr	V	Y	Zr	Ga	U[1]	Th[1]
Geometric means and geometric deviations of analyses of 216 lower Eocene sandstone samples																
Geometric mean	144	13	415	4.3	13	8.1	12	8.5	7.6	138	24	9.6	113	8.9	2.44	4.28
Geometric deviation	3.71	1.8	2.2	2.3	2.7	1.9	1.7	2.0	2.0	2.6	1.9	2.3	1.8	1.8	1.58	2.02
Geometric mean × GD	534	23.4	913	9.9	35.1	15.4	20.1	17.0	15.2	359	46	22	203	16	3.86	8.65
Geometric mean ÷ GD	39	7.2	189	1.9	4.8	4.3	6.9	4.3	3.8	53	10.4	4.2	63	4.9	1.54	2.12
Geometric means of analyses of six samples from each of 36 areas																
Locality (area in fig. 1)																
Bighorn Basin, Wyo.:																
Enos Creek (1)	175	.....	250	10	37	12	.....	26	11	108	22	16	93	9.8	*1.71	*6.25
Hillberry Rim (2)	36	41	279	3.2	6.8	9.0	.....	7.8	6.4	31	26	11	241	.....	*2.12	*4.28
Fossil basin, Wyo.:																
Evanston (3)	201	13	289	7.8	29	10	.....	13	.....	129	29	19	121	.....	.....	.....
Fossil (4)	229	.....	189	10	9.2	7.8	.....	8.1	8.3	98	20	14	96	.....	*3.37	*3.64
Galisteo basin, N. Mex.:																
Cerrillos (5)	98	12	376	2.6	3.9	6.0	.....	4.5	6.4	73	14	.....	105	.....	*.92	*2.28
Hagen (6)	133	.....	757	6.1	5.7	8.4	.....	5.3	.....	186	31	.....	74	11	*1.06	*3.94
Great Divide Basin, Wyo.:																
Oregon Buttes (7)	1022	16	529	12	44	14	.....	24	6.5	362	60	9.0	93	15	*2.43	*4.42
Crooks Gap–Wamsutter (8)	65	.....	418	2.8	6.5	6.1	13	5.8	22	79	18	6.6	91	18	*4.41	*13.80

TABLE 7. — *Distribution of constituents in 216 samples of lower Eocene sandstone and in 36 areas and four color subsets of the samples — Continued*

	Minor elements, in parts per million															
	Mn	B	Ba	Co	Cr	Cu	Ti	Ni	Pb	Sr	V	Y	Zr	Ga	U[1]	Th[1]
Geometric means of analyses of six samples from each of 36 areas—Continued																
Green River Basin, Wyo.:																
La Barge (9)	349	13	550	7.6	53	10	18	21	8.5	435	45	15	201	15	*4.31	*14.41
Firehole Basin (10)	442	16	393	7.9	37	10	13	19	8.4	207	36	12	146	9.6	*2.04	*7.22
Hanna basin, Wyo.:																
Difficulty (11)	24	.....	405	.....	4.0	4.1	.....	.....	.....	88	10	.....	66	5.6	*2.26	*2.14
Carbon basin (12)	223	13	331	4.8	21	6.3	19	8.3	6.6	127	27	12	150	11	*.91	*4.16
Hoback–western Wind River Basins, Wyo.:																
Dubois (13)	202	.....	398	5.0	39	7.8	15	17	8.2	263	31	8.4	93	12	.....	.....
Hoback basin (14)	371	.....	382	7.9	24	8.4	13	10	6.4	128	29	16	108	9.2	*2.45	*3.97
Piceance Creek basin, Colo.:																
Rangely (15)	134	20	281	2.6	9.5	6.0	13	6.6	8.2	113	22	8.0	139	6.0	*1.82	*4.24
Battlement Mesa (16)	92	12	486	3.6	6.5	7.4	15	5.9	6.3	70	23	6.9	189	8.2	*1.24	*5.36
Powder River Basin, Wyo.:																
Pine Ridge–Pumpkin Buttes (17)	37	23	505	3.2	7.9	5.8	.....	4.2	8.2	57	21	10	178	7.3	2.07	5.61
Horse Creek–Crazy Woman Creek (18)	483	.....	302	6.4	24	11	.....	12	.....	190	30	19	103	7.9	2.11	6.18
Raton basin, Colo.:																
Huerfano Park (19)	254	.....	1254	4.0	11	11	.....	7.0	7.9	251	32	.....	80	16	.93	3.50
West Spanish Peak (20)	217	.....	378	.....	10	13	.....	8.8	6.3	165	28	8.4	93	13	1.97	5.46
Sand Wash basin, Colo.:																
Little Snake River (21)	113	.....	600	2.5	9.4	4.3	20	5.5	18	164	17	8.8	91	10	3.12	13.24
Elkhead Mountains (22)	48	17	568	3.6	8.0	6.8	.....	6.3	6.3	98	32	.....	104	8.1	1.86	5.13
San Juan Basin, N. Mex.:																
Cuba (23)	42	.....	427	.....	3.7	4.1	13	3.9	.....	56	11	7.2	74	6.7	*1.88	*2.65
Gobernador (24)	301	.....	897	4.4	9.6	5.8	.....	8.3	8.1	217	33	7.9	127	11	*3.19	*4.45
Shirley Basin, Wyo.:																
Bates Hole (25)	50	.....	712	2.5	5.5	5.4	14	5.5	6.3	218	24	.....	75	14	6.78	29.22
Chalk Hills (26)	25	.....	448	.....	.....	4.5	18	.....	19	77	10	6.4	102	11	3.28	17.51
Uinta Basin, Utah:																
Soldier Summit (27)	437	.....	1500	9.7	24	16	.....	12	8.5	178	48	18	135	13	*3.22	*10.32
Patmos Head (28)	381	19	740	9.4	37	24	17	19	18	246	84	8.8	145	14	*2.20	*8.86
Wasatch Plateau, Utah:																
Salina (29)	159	.....	419	3.2	6.3	8.3	.....	4.1	.....	731	12	6.4	118	.....	*2.84	*2.72
Gunnison Plateau (30)	146	31	388	3.2	14	11	13	11	.....	203	27	8.7	207	9.0	*2.13	*7.66
Wasatch Range, Utah:																
Woodruff (31)	80	18	64	4.3	17	8.1	.....	8.1	.....	56	11	19	129	.....	* .61	*0.72
Morgan (32)	241	.....	150	4.4	16	7.0	.....	7.7	.....	86	14	27	82	5.7	*1.27	*2.62
Washakie Basin, Wyo.:																
Baggs (33)	178	16	408	3.6	23	13	.....	11	8.1	146	38	15	127	9.6	*2.84	*7.59
Erickson–Kent Ranch (34)	233	21	403	2.5	19	6.4	.....	8.4	.....	192	24	11	141	7.6	*2.86	*8.06
Wind River Basin, Wyo.:																
Lost Cabin (35)	189	20	227	4.8	27	11	13	12	10	117	20	14	132	8.2	2.28	4.22
Wallace Creek (36)	61	.....	630	2.7	16	8.2	.....	12	15	143	20	6.9	57	14	6.52	11.46
Geometric means of analyses of samples from four subsets grouped on the basis of color																
40 red sandstones	172	14	451	4.1	12	9.6	10	7.5	6.7	117	23	10	116	8.7	.....	.....
67 orange sandstones	151	13	341	3.8	11	7.1	11	8.1	7.0	133	21	8.9	110	7.7	.....	.....
98 yellow sandstones	117	13	437	4.2	13	7.7	13	8.1	8.1	133	25	9.5	108	9.3	.....	.....
11 green sandstones	396	20	632	10	54	17	16	27	11	394	58	13	174	17	.....	.....

	Minerals, in inches of deflection								
	MLC	Mica	Kaolin	Quartz	Potassium feldspar	Plagio-clase	Calcite	Dolomite	Zeolite
Geometric means and geometric deviations of analyses of 216 lower Eocene sandstone samples									
Geometric mean	0.008	0.06	0.06	1.74	0.49	0.16	0.04	0.013	0.002
Geometric deviation	18	13	15	1.5	14	26	40	29	5
Geometric mean × GD	.143	.775	.880	2.54	7.09	4.22	1.62	.375	.019
Geometric mean ÷ GD	.0004	.0046	.0041	1.19	.034	.006	.0009	.0004	.0004
Geometric means of analyses of six samples from each of 36 areas									
Locality (area in fig. 1)									
Bighorn Basin, Wyo.:									
Enos Creek (1)	.....	0.033	0.83	1.93	0.22	0.006	0.014	0.059	.....
Hillberry Rim (2)	.....	.013	.095	2.59	.052	.....	.....	.....	.....
Fossil basin, Wyo.:									
Evanston (3)	.....	.21	.19	1.71	.079	.....	1.92	.87	.....
Fossil (4)	.....	.014	.27	2.29	.010	.13	1.94	1.12	.....
Galisteo basin, N. Mex.:									
Cerrillos (5)	.....	.003	.42	2.46	.35	.038	.14	.....	.....
Hagen (6)	.22	.014	.007	1.43	2.03	1.19	.007	.....	.....
Great Divide Basin, Wyo.:									
Oregon Buttes (7)	.002	.50	.016	1.35	2.48	2.79	.18	.009	.....
Crooks Gap–Wamsutter (8)	.13	.46	.14	1.41	3.59	2.02	.009	.008	.....
Green River Basin, Wyo.:									
La Barge (9)	.....	.76	.011	1.31	.34	.20	.11	.13	0.019
Firehole Basin (10)	.002	.54	.11	1.64	.90	1.59	.26	.16	.002
Hanna basin, Wyo.:									
Difficulty (11)	.....	.083	.066	1.65	3.77	1.84	.004	.....	.....
Carbon basin (12)	.....	.26	.68	1.62	.45	.26	.033	.033	.....
Hoback–western Wind River Basins, Wyo.:									
Dubois (13)	.071	.25	.095	1.23	.39	.43	.48	.14	.....
Hoback basin (14)	.051	.077	.34	1.78	.24	.25	.55	.069	.....
Piceance Creek basin, Colo.:									
Rangely (15)	.018	.015	.052	2.55	.81	.095	.28	.12	.....
Battlement Mesa (16)	.14	.013	.52	2.36	1.82	.33	.007	.....	.....
Powder River Basin, Wyo.:									
Pine Ridge–Pumpkin Buttes (17)	.003	.21	.....	2.53	1.17	.016	.....	.....	.004
Horse Creek–Crazy Woman Creek (18)	.....	.42	.37	.93	.22	.018	1.74	.13	.....
Raton basin, Colo.:									
Huerfano Park (19)	.17	.070	.19	1.72	4.93	.88	.003	.....	.....
West Spanish Peak (20)	.070	.020	.006	1.94	.32	2.95	.....	.....	.23
Sand Wash basin, Colo.:									
Little Snake River (21)	.18	.49	.066	1.78	3.56	1.08	.008	.....	.....
Elkhead Mountains (22)	.010	.030	.092	2.03	1.72	.077	.....	.....	.....
San Juan Basin, N. Mex.:									
Cuba (23)	.003	.014	.17	2.22	1.50	.040	.....	.....	.....
Gobernador (24)	.....	.002	.002	1.60	2.03	4.00	.024	.....	.....

TABLE 7. — *Distribution of constituents in 216 samples of lower Eocene sandstone and in 36 areas and four color subsets of the samples*—Continued

	Minerals, in inches of defection								
	MLC	Mica	Kaolin	Quartz	Potassium feldspar	Plagioclase	Calcite	Dolomite	Zeolite
Geometric means of analyses of six samples from each of 36 areas—Continued									
Shirley Basin, Wyo.:									
Bates Hole (25)	0.020	0.28	0.006	1.41	4.70	3.41	.....	.....	.....
Chalk Hills (26)	.009	.083	.092	1.91	4.71	.10	.....	.....	.....
Uinta Basin, Utah:									
Soldier Summit (27)	.29	.19	.76	1.63	.035	1.07	2.00	1.59	.....
Patmos Head (28)	.037	.28	.017	1.25	.53	.43	.083	.54	0.20
Wasatch Plateau, Utah:									
Salina (29)	.013	.013	.005	2.05	.10	.014	2.17	1.08	.....
Gunnison Plateau (30)	.14	.13	.033	1.87	.65	1.64	.037	.003	.006
Wasatch Range, Utah:									
Woodruff (31)	.002	.....	.046	1.70	.....	.....	.27	.008	.....
Morgan (32)	.....	.015	.35	1.45	.021	.....	3.94	.14	.....
Washakie Basin, Wyo.:									
Baggs (33)	.008	.033	.032	1.77	.77	.26	.042	.....	.....
Erickson–Kent Ranch (34)	.....	.46	.28	1.59	1.18	1.26	.14	.025	.....
Wind River Basin, Wyo.:									
Lost Cabin (35)	.008	.064	.007	2.00	.12	.010	.17	.093	.....
Wallace Creek (36)	.003	.23	.015	1.62	4.18	2.90	.002	.003	.....
Geometric means of analyses of samples from four subsets grouped on the basis of color									
40 red sandstones	0.019	0.028	0.075	1.84	0.17	0.063	0.064	0.012	0.003
67 orange sandstones	.004	.023	.043	1.87	.35	.11	.051	.015	.001
98 yellow sandstones	.008	.14	.089	1.69	.93	.24	.027	.011	.001
11 green sandstones	.013	.89	.009	1.22	.58	1.99	.062	.024	.008

[1]Uranium and thorium data based on a total of only 86 samples analyzed.
*Single sample.

in the distribution of the original data. The distribution patterns of the different constituents vary greatly among the sample areas. Much of this variation may arise because six samples cannot give a very complete picture of the distribution patterns. In the color subsets, the distribution patterns are similar to those shown in the complete set of 216 samples.

For the 216 lower Eocene sandstone samples, the concentration range of the major elements or oxides is shown in figure 15, and that of the minor elements is shown in figure 16. For comparison, on both figures we plotted the mean values for an average sandstone as estimated by Pettijohn (1963, p. S11, S15). Pettijohn computed his average from selected published analyses after estimating that the average sandstone would include 26 parts graywacke, 25 parts lithic sandstone, 15 parts arkose, and 34 parts orthoquartzite. Pettijohn's averages closely correspond to the means computed for the lower Eocene sandstones for SiO_2, Al_2O_3, CaO, K_2O, H_2O-, H_2O+, CO_2, Ba, Cr, Cu, Ga, Pb, and V. Total iron as Fe_2O_3, MgO, Na_2O, TiO_2, P_2O_5, MnO, B, and Zr are less in the lower Eocene sandstones than in the average sandstone. Co, La, Ni, Sr, Y, Th, and U are greater in the lower Eocene sandstone than in the average sandstone. Many replacement values in the data sets for B, Co, La, Pb, and Y (table 6) and the small number of analyses for U and Th reduce the accuracy for those elements. The two sets of values probably reflect similarities and differences in provenance, lithologic types, environments of deposition, and diagenetic history.

To check whether distinctive groups of minor elements might characterize certain end-member types of sandstone, subsets of samples were chosen in which the mean of one mineral constituent exceeded by one standard deviation the arithmetic mean of that constituent in the total set of 216 samples. The mean value was calculated for each constituent in these subsets and was compared with the mean value for the full set of 216 samples. No unusual concentrations of minor elements were found in any of these end-member types of sandstone. Additional subsets were chosen in which a combination of two minerals was highly concentrated or in which one mineral was very low, and still no unusual concentrations of minor elements were found. This seems to indicate that the distribution of minor elements is independent of the major-mineral composition of the samples. Perhaps the minor-element distribution is affected more by diagenesis, provenance, and weathering than by the proportion of major-mineral constituents.

This indication is further supported by the differences between the geometric means of four color subsets. The 216 samples were distributed as follows: 40 red, 67 orange, 98 yellow, and 11 green.[2] The distribution of the colors is shown in figure 5, and the number of samples from each section in each color subset is listed in table 1.

Little is known about the geochemical significance of color, although iron oxides are commonly regarded as the principal coloring agent in sandstones.

[2]Colors are based on ground sample color and were arbitrarily selected from the "Rock-Color Chart" of Goddard and others (1948) as follows: Red, 10*R* 6/2, 10*R* 6/6, 10*R* 7/4, 7*R* 7/4, 10*R* 5/4, 5*YR* 8/1, 5*YR* 7/2, 5*YR* 8/4, 5*R* 8/1; orange, 10*YR* 8/2, 10*YR* 7/4, 10*YR* 8/6, 10*YR* 7/6, 10*YR* 6/4, 5*YR* 5/6, 5*YR* 4/1, 5*YR* 6/4; yellow, 5*Y* 7/2, 5*Y* 8/1, 5*Y* 8/4, 5*YR* 6/1, *N*8, *N*9; green, 5*Y* 7/1, 5*Y* 6/1, 5*Y* 5/2, 5*GY* 7/2, 5*GY* 8/1, 5*G* 8/1, 10*Y* 8/2.

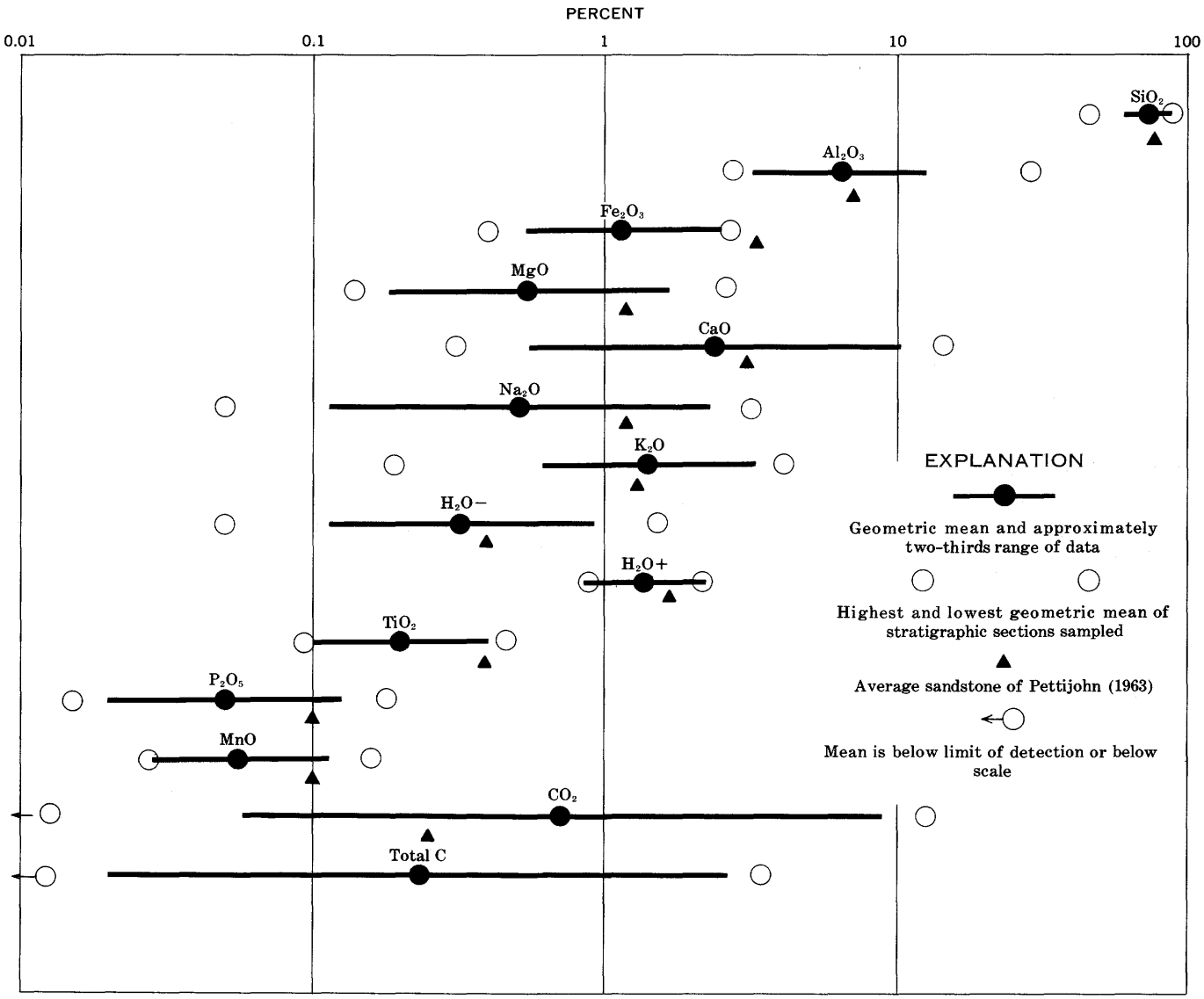

FIGURE 15. — Concentration range of major constituents in 216 samples of lower Eocene sandstone in the Rocky Mountain region.

The color is related more to the oxidation state of the iron and to the mineralogy of the iron oxide and hydrate minerals than to the amount of iron (Walker, 1967). Among the lower Eocene sandstones, the red sandstone subset contains less total iron than any of the other three color subsets. The green sandstone subset contains nearly 2½ times as much total iron as the red sandstone subset and more of every constituent except SiO_2, quartz, "mixed layer clay," "kaolin," potassium feldspar, and calcite than any of the other three subsets (table 7). In the green sandstone samples, the geometric means of cobalt, chromium, copper, nickel, strontium, vanadium, gallium, and "mica" each exceed the geometric mean of the 216 samples by at least one geometric deviation. The mean peak height of "mica" in the green sandstone subset is about 15 times higher than the mean of the 216 samples and is more than 6 times higher than the mean of the yellow subset. This high "mica" content may be related to the abundance of iron and minor elements in the green sandstones: by lowering the permeability of the green sandstones the "mica" could prevent the leaching of iron and minor elements by oxidizing solutions. Also, micas can contain higher concentrations of some minor elements, including barium, manganese, chromium, titanium, and vanadium (Deer and others, 1962, p. 31, 61), than can most other common sandstone minerals such as quartz, feldspars, calcite, or kaolin, although micas in general do not scavenge minor elements as readily as do other clay minerals or organic minerals. Greenish mica may be partly responsible for the

color of some of the sandstone samples, although green chlorite and epidote are also present in some of the samples.

As can be seen in figure 5, the green color is not closely related to provenance or to sandstone type. The green sandstone samples were mostly intermediate, but two were carbonate rich, and one was feldspar rich. Green sandstone was collected in the Green River Basin, Great Divide Basin, Bighorn Basin, Wind River Basin, and the Wasatch Plateau, and green-tinted sandstone was noticed in some of the other basins. Both crystalline and sedimentary terranes were contributing debris to these areas (fig. 1). Possibly the development and preservation of the green color and the abundance of minor elements are related to the depositional environments, but more likely the color was produced by diagenetic alteration. This would explain abrupt color changes commonly observed along a single bed and among beds in stratigraphic sequence. However, more investigation is needed before all the factors influencing color can be evaluated.

GEOCHEMICAL RELATIONS

ANALYSIS OF VARIANCE

The four-level hierarchial sampling plan previously described was designed to allow use of analysis of variance in evaluating the relative importance of differences in element and mineral concentrations as functions of geographic or stratigraphic position. The computer program follows the computational technique of Anderson and Bancroft (1952). We used a four-level nested model in the analysis of variance, similar to the model used by Krumbein and

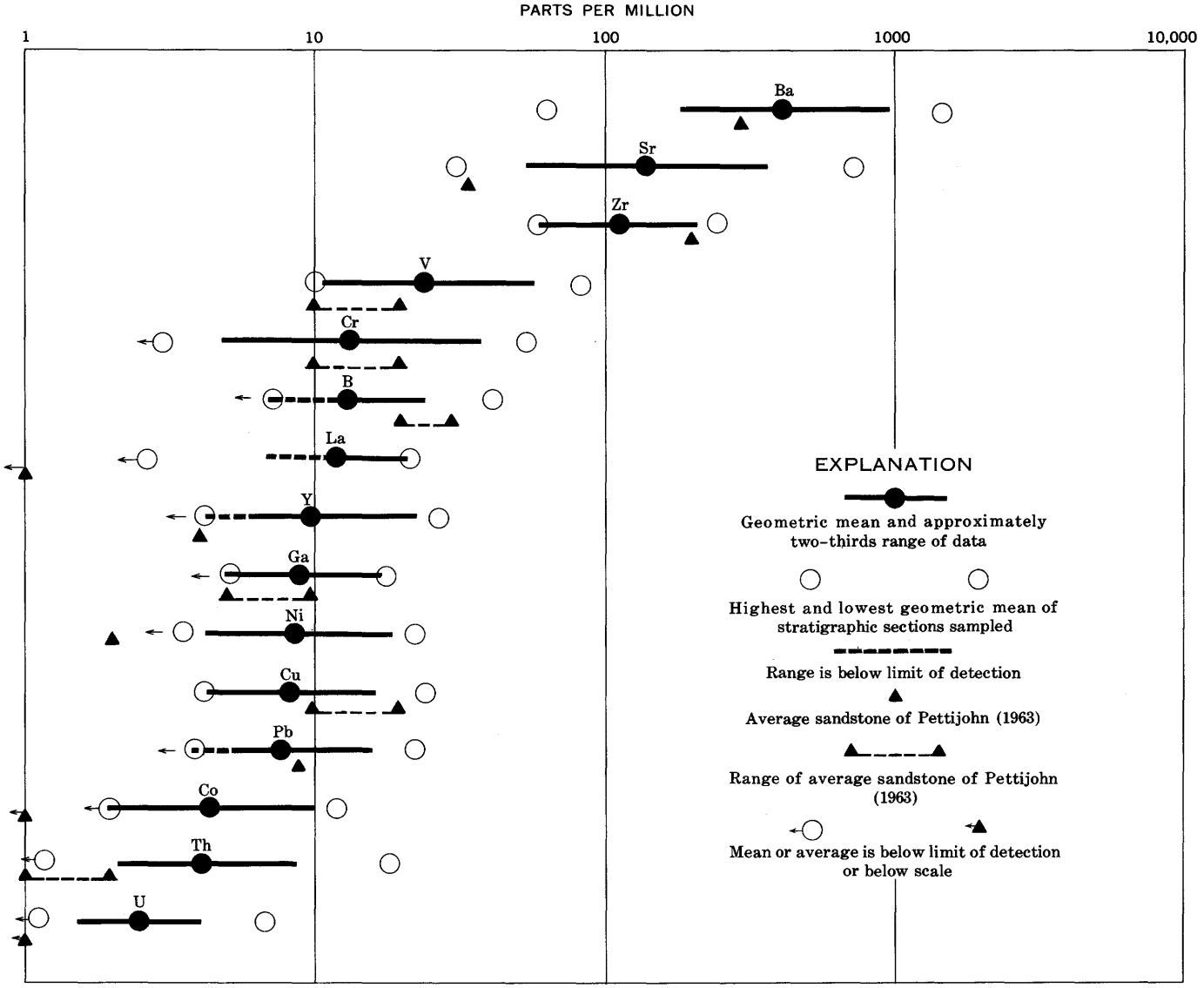

FIGURE 16. — Concentration range of minor elements in 216 samples of lower Eocene sandstone in the Rocky Mountain region.

Slack (1956) except that the distance between levels could not be held constant. The computations were made on the log-transformed data. Constituents having many indeterminate values (table 6) are not included in this discussion. Table 8 lists the percentage of variance components at each of the four levels.

The following constituents show significant variance between basins: Al_2O_3, total iron as Fe_2O_3, Na_2O, K_2O, H_2O-, Ba, Cr, Cu, Ni, "mica," and potassium feldspar. All the constituents tested except total iron, Cu, and "mica" show significant variance between sections within basins, and all except total iron, TiO_2, MnO, Ni, and Zr show significant variance between paired beds within sections. All the constituents except plagioclase, for which no test of the significance was made, show a large percentage of the total variance between samples. Al_2O_3, "mica," and potassium feldspar show their greatest percentage of variation at the basin level. MgO, CaO, Na_2O, K_2O, and CO_2, "kaolin," and plagioclase show the greatest variation at the section level. Considered together, these two levels indicate significant regional variations in the feldspars and carbonate minerals that are mappable, as shown in figure 5. Sr shows the greatest variation between paired beds within sample areas, which probably reflects the extremely high Sr contents (due to celestite cement) of several samples from the Salina area (table 1). The remaining constituents all show their greatest variation between samples.

The variance between samples has several causes. Analytical error is included at this level, but, as can be seen from table 2, the analytical error is a small part of the total variance between samples for most constituents. Variance at this level also reflects the effects of microgeochemical environments; for example, the high variance shown by TiO_2 and Zr may be partly due to differences in concentrations of heavy minerals, such as zircon and ilmenite, that commonly occur in a single bed. The variance of total iron and MnO could reflect differences in the degree of weathering of the samples and differences in diagenetic alteration due to unequal porosities of two beds. The variance between pairs of beds can be explained by local environmental differences at the sites of deposition or by changes resulting from progressive erosion of the source terrane. The variance shown by the two lower levels of the sampling plan may be regarded as "back-

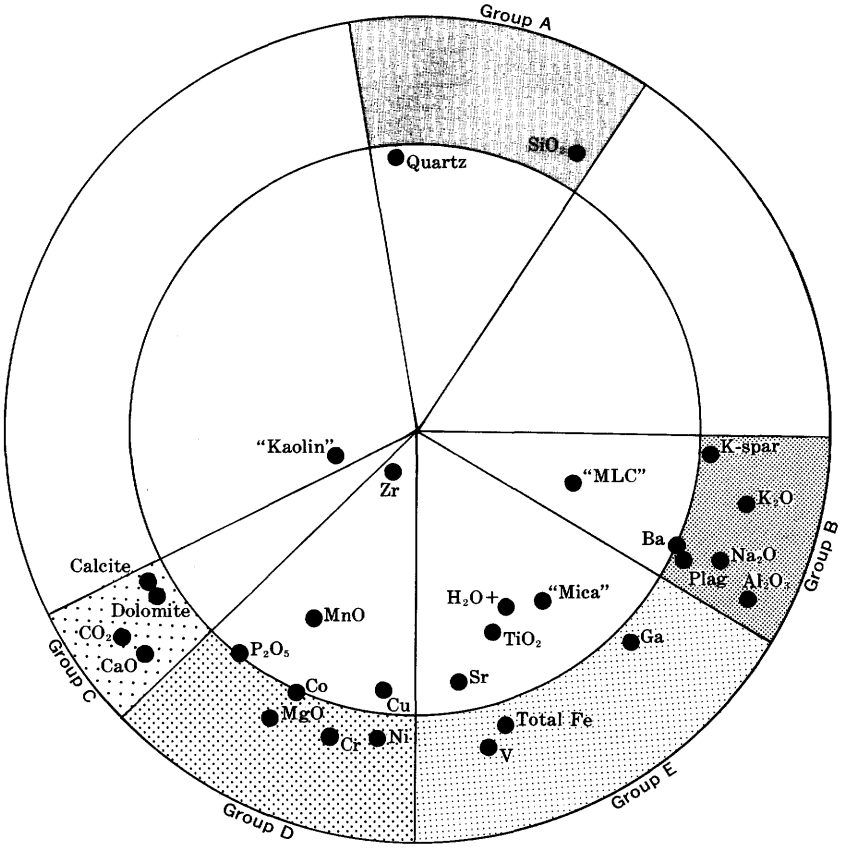

FIGURE 17. — Vector diagram for 216 samples of lower Eocene sandstone. "K-spar" is potassium feldspar, "Plag" is plagioclase, and "MLC" is mixed layer clays.

ground noise" that masks some or all of the regionally significant geochemical trends.

TABLE 8. — *Variance components (in percent)*

[Numbers in italic indicate significant variance at the 95-percent level. Note that no test for significance was made at the lowest level, between samples within paired beds]

Variance components	Between basins within region	Between sections within basins	Between paired beds within sections	Between samples within paired beds
SiO_2	0	*35.6*	*25.8*	38.6
Al_2O_3	*33.7*	*20.8*	*20.5*	24.7
Fe_2O_3[1]	*15.0*	9.9	11.7	63.4
MgO	16.5	*38.1*	*8.1*	37.3
CaO	6.2	*41.1*	*18.1*	34.6
Na_2O	*25.3*	*28.0*	*21.0*	25.8
K_2O	*25.4*	*29.2*	*19.8*	25.6
H_2O+	8.5	*12.0*	10.6	68.9
H_2O-	*30.9*	*16.9*	*13.9*	38.3
TiO_2	6.3	*15.1*	0.8	77.9
P_2O_5	17.9	*27.2*	*14.4*	40.6
MnO	1.4	*16.3*	3.1	79.2
CO_2	15.5	*33.6*	*17.6*	33.3
Ba	*27.5*	*15.7*	*14.3*	42.5
Cr	*28.6*	*30.0*	*11.4*	30.4
Cu	*24.3*	4.7	*12.9*	58.2
Ni	*24.0*	*30.1*	3.7	42.3
Sr	12.8	*21.8*	*40.1*	25.3
V	19.7	*27.9*	*14.3*	38.2
Zr	1.2	*15.8*	4.0	79.0
"Mica"	*33.9*	9.1	*25.5*	31.5
"Kaolin"	0	*40.3*	*26.3*	33.4
Quartz	10.7	*22.8*	*17.4*	49.1
K-feldspar	*32.6*	*23.9*	*14.6*	28.8
Plagioclase	20.2	*34.2*	*27.6*	18.0

[1]Total iron as Fe_2O_3.

The variance components in table 8 show significant differences between basins for all of the constituents that could be tested in the lower Eocene sandstones. This indicates that, for most constituents, the sampling plan was reasonably adequate and that not much more information would have been gained from a few more samples. The feldspar minerals and their component constituents, Al_2O_3, K_2O, and Na_2O, show about the same variance between sample areas as they do between basins. Constituents that show significant variation between sample areas but not between basins include P_2O_5; those constituents that occur in resistate minerals (including SiO_2, quartz, Zr, and TiO_2), those that form carbonate minerals (CaO, MgO, and CO_2). SiO_2 and quartz are probably so ubiquitous that an unreasonably large number of samples would be required to define variation at the basin level. Variance percentages for P_2O_5, Zr, TiO_2, and the carbonate-mineral components probably reflect a greater difference between source areas for different sample areas within the same basin than between basins within the region. Another group, including Fe_2O_3, Cu, and "mica," shows significant variance between basins, but not between sections. This indicates that the principal regional variation is on a very large scale and that additional samples would be required to define the variance between sample areas.

COMPONENT ANALYSIS

Component analysis of correlation data supplements the interpretation of geochemical associations of the various constituents detected. The technique used is similar to that previously described in a geochemical study of black shales (Vine and Tourtelot, 1969, p. A11–A12; 1970b). Component analysis, as described by Harman (1960), Imbrie and VanAndel (1964), Griffiths (1966), and Miesch, Chao, and Cuttitta (1966), involves constructing radial vectors for each constituent so that the cosine of the angle between any two vectors is equal to the coefficient of correlation. The vectors are then rotated and projected onto a two-dimensional diagram on which varimax axes are selected that will best represent the data. In these vector diagrams, the radial lines are omitted, and the position of each constituent is shown within a circle of unit radius. Segments of the diagram are patterned to suggest possible geochemical groupings of the constituents. The illustrations can be readily compared for geochemical interpretations. Constituents that plot close together near the outer rim of the circle usually have significant positive correlations with each other. Constituents that plot close together near the center of the circle have short vectors, indicating a large angle with the plane of projection, and may or may not have significant correlations with each other. Constituents that plot on opposite sides of the circle have strong negative correlations; those that plot at right angles from each other show no correlations. Short vectors that are poorly represented on the two-dimensional plot may be close together or far apart on a three-dimensional plot.

Correlation data that are part of a closed array (the sum of the parts equals 100 percent) have certain inherent biases, as described by Chayes (1960), that cannot be avoided. For example, if a rock has three principal constituents, there must necessarily be a negative correlation between the predominant constituent and the other two. A positive correlation may be imposed on certain pairs of minor constituents, even though there is no geochemical association between the pairs, because they both vary inversely with the predominant constituent. However, in our experience, the technique is both useful and valid because it leads to geochemical interpretations that are for the most part reasonable and consistent with geochemical theory.

Figure 17 shows a vector diagram constructed from principal-component analysis of the correlation matrix for 29 constituents in the 216 samples of lower Eocene sandstones from the Rocky Mountain region. Eigenvalues show that about 50 percent of the variation in the data is represented. This low representation is probably partly due to the variety of sandstone types included in the sample set. However, the representation is sufficient to give a gross

picture of the geochemical relations. The array of points on the diagram may be divided into three major and two minor groups, as indicated by the patterned areas. Near the top of the diagram is a group (A) composed of quartz and SiO_2. The separation of the points representing these two constituents is mostly a function of the amount of SiO_2 in minerals other than quartz, although the separation may also reflect some bias in the X-ray data. An inverse correlation between this group and the other four groups is an indication of the predominance of quartz over other minerals and illustrates the problem of closure. On the lower right side of the diagram is a segment characterized by potassium feldspar, plagioclase, K_2O, Na_2O, Al_2O_3, and barium, referred to as the feldspar group (B). On the left side is a segment referred to as the carbonate group (C) that includes calcite, dolomite, CO_2, and CaO. Most of the remaining constituents are scattered between the carbonate and feldspar groups. The segment adjacent to the carbonate group is designated group D and includes P_2O_5, MnO, MgO, Co, Cr, Ni, and Cu. The segment adjacent to the feldspar group contains total iron, "mica," Ga, H_2O+, TiO_2, Sr, and V and is designated group E. Group D is probably more closely related to the carbonate group, and group E to the feldspar group, although there is not unequivocal separation of all constituents. Groups D and E tend to correlate with each other as well.

Vector diagrams (fig. 18) were constructed for each of the four color subsets previously described (p. 23). Although these diagrams and the vector diagram for the 216 samples (fig. 17) are generally similar, certain differences are evident that may have geochemical significance. The vector diagram for the red sandstones (fig. 18*A*) shows a closer correlation of "mica," "MLC," and TiO_2 with the feldspar group and Cu and Sr exchange places in groups D and E as compared with their positions in the 216 sandstone samples. The differences between the two diagrams are partly a result of greater homogeneity among the red sandstone samples than among the samples in the complete set. For example, in the vector diagram for the red sandstones, group E may represent mostly the constituents found in the hematite that gives the color, whereas in the vector diagram for the 216 variously colored sandstones, group E includes constituents of a variety of hydrous iron oxide minerals. The close association of V and Cu with iron (fig. 18*A*) suggests that these two elements occur almost exclusively in the iron oxide minerals in the red sandstones, whereas in the 216 sandstones Cu must occur in other constituents as well, as suggested by its position in group D (fig. 17).

For the orange subset the vector diagram (fig. 18*B*) is most like that of the whole set and represents a similar mixture of sandstone types, as indicated in figure 5.

For the yellow subset (fig. 18*C*), which contains the most samples of the four subsets, the vector diagram shows some major differences when compared with the diagram for the entire group of samples. Group D includes the calcite group, and group E has moved away from the feldspar group and is almost indistinguishable from the calcite group. Ga is in group B rather than group E and is more definitely associated with the feldspar group. Several constituents, including Zr, "kaolin," TiO_2, H_2O+, and "mica", show no close association with any of the groups. Inspection of the correlation coefficients reveals that Zr tends to correlate positively with both quartz and TiO_2 at the 99-percent confidence level. "Kaolin" shows positive correlations with calcite and dolomite; TiO_2, with Zr and with total iron; and H_2O+, with group E constituents. "Mica" shows no significant positive correlations. The yellow subset is composed principally of very faintly colored samples. Although the content of total iron (table 7) is close to that of the whole set of 216 samples and to that of the orange subset, both color and correlation statistics suggest that, in the yellow subset, the content of iron oxide minerals may be significantly lower and that more of the iron occurs in carbonate minerals than in iron oxide minerals. Sr seems to be the only element that occurs about equally in the carbonate group and in the feldspar group. The position of Ga in the feldspar group also suggests a decrease in iron oxide minerals. Ga may occur in iron oxide minerals and, more likely, in aluminum minerals such as the feldspars (Goldschmidt, 1954, p. 327). Inspection of the correlation coefficients and of the vector diagram suggests that, in the yellow sandstones, the minor elements, except Ba, Ga, and part of the Sr, occur more with carbonate and phosphate minerals (probably mostly the dolomite) than with the iron oxide minerals, whereas in the orange and red subsets, they occur more with the iron oxide minerals.

For the green subset the vector diagram (fig. 18*D*) is distinctly different from that of the other subsets. The three major groups—quartz, feldspar, and carbonate—retain their same general orientation with respect to each other, but group E has disappeared, and group D has lost most of its constituents and is on the other side of the calcite group. A new group, F, composed of total iron, Cu, "kaolinite," "MLC," and H_2O+, can be differentiated next to group D, but the strong correlation shown by total iron with "kaolin," "MLC," and H_2O+ in group F suggests

that most of the iron occurs in micaceous and clay minerals. Groups D and F are inversely related to the feldspar group. Potassium feldspar is positioned near the quartz group, perhaps reflecting a predominance of plagioclase over potassium feldspar (table 7). Many constituents fall close to the center of the circle and show no strong association with any group. The general scattering of those constituents means partly that 11 samples are insufficient for correlation statistics and partly that, in the green subset, the elements are partitioned differently among the major constituents than in the other subsets. For instance, the correlation coefficients show that Co has a positive correlation with potassium feldspar at the 99-percent confidence level. Some elements—for example Ga, Sr, and MnO—are about equally associated with two inversely related groups. The correlation coefficients are below the 90-percent confidence level for any positive correlations for K_2O and Ba. Other elements—for example Ni and V—show strong positive correlations only between each other. The inverse relation of group F to the feldspar group suggests that the constituents of group F may replace plagioclase diagenetically in the green sandstone.

GEOCHEMISTRY OF SAMPLE AREAS

Table 9 lists areas that are rich in various constituents; the areas and constituents are grouped in a sequence suggested by geochemical similarities.

TABLE 9. — *Areas where any constituent mean value for six samples is greater than one geometric mean times the geometric deviation of all samples (+) or is less than one geometric mean divided by the geometric deviation of all samples (●)*

AREA (figure 1)	CONSTITUENT																												
	Quartz	SiO_2	Zr	B	TiO_2+Ti	Al_2O_3	Na_2O	K_2O	Ga	Pb	"MLC"	Ba	Total Fe	MnO	Sr	Cr	Ni	V	Co	Cu	MgO	Dolomite	Co_2+total C	Calcite	CaO	P_2O_5	Zeolite	"Kaolin"	K-spar	Plagioclase
2. Hillberry Rim	+	+	+								●			●	●		●							●	●					
23. Cuba		+															●		●		●			●		●				
17. Pine Ridge-Pumpkin Buttes		+		+			●		●															●	●			●		
30. Gunnison Plateau			+	+	+																									
25. Bates Hole						+	+	+																●						
24. Gobernador							+				●																	●		
26. Chalk Hills								+								●	●	●	●		●			●						
8. Crooks Gap-Wamsutter								+	+															●						
19. Huerfano Park								+	+															●						
36. Wallace Creek				●			+	+		+	+	+												●	●	●				
21. Little Snake River										+	+								●					●	●					
6. Hagen											+													●						
28. Patmos Head					+		+			+			+			+	+	+		+	+	+					+			
1. Enos Creek											●		+			+	+		+											
7. Oregon Buttes													+	+	+	+	+	+	+											
27. Soldier Summit											+	+								+	+	+		+						
9. La Barge															+	+	+													
10. Firehole Basin																+	+													
13. Dubois																+	+				+									
29. Salina						●			●				●		+		●					+	+	+						
4. Fossil						●		●	●		●								+				+	+	+	+			●	
32. Morgan		●				●	●	●			●												+	+	+				●	●
18. Horse Creek-Crazy Woman Creek	●	●									●												+	+	+	+				
3. Evanston						●	●		●		●												+	+						●
20. West Spanish Peak																								●			+			
22. Elkhead Mountains																								●	●					
5. Cerrillos											●		●			●			●		●			●		●				
11. Difficulty									●		●					●	●	●	●	●	●				●	●				
31. Woodruff						●	●	●	●			●	●								●								●	●

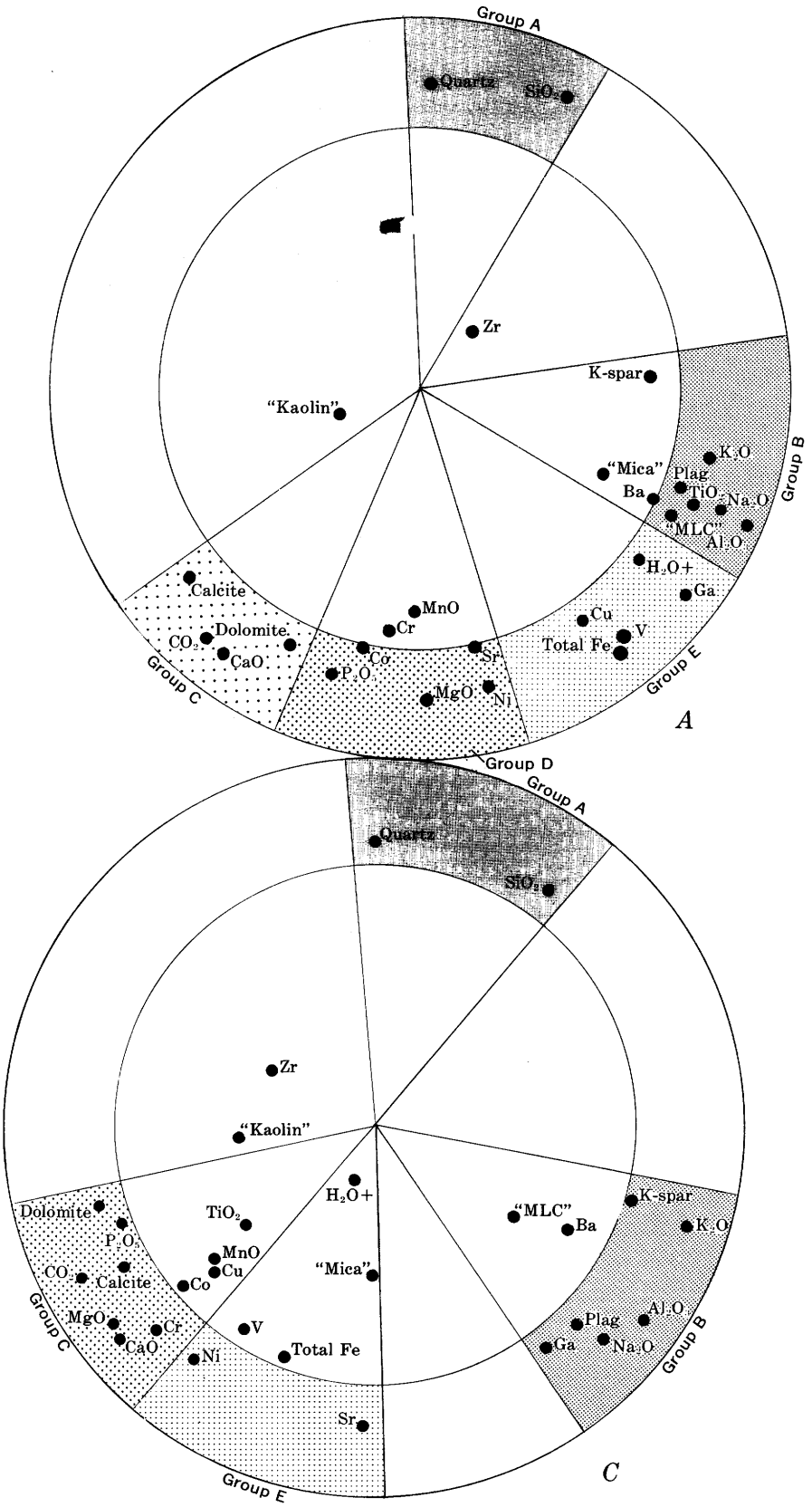

FIGURE 18. — Vector diagrams for color subsets of the sandstone samples: feldspar, "Plag" is plagioclase,

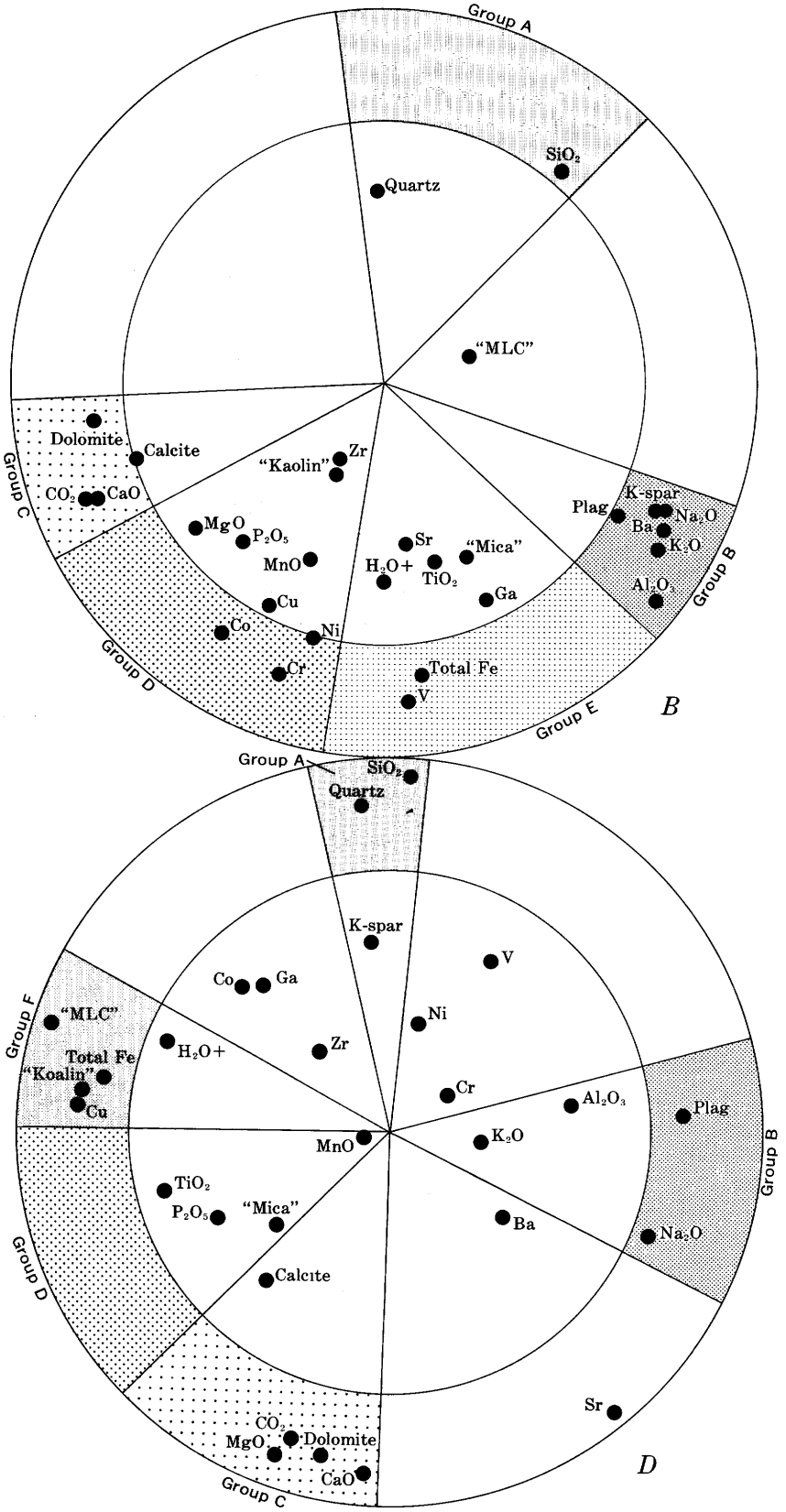

A, 40 red; *B*, 67 orange; *C*, 98 yellow; *D*, 11 green. "K-Spar" is potassium and "MLC" is mixed layer clays.

Ahrens, L. H., 1954, The lognormal distribution of the elements (a fundamental law of geochemistry and its subsidiary): Geochim. and Cosmochim. Acta, v. 5, no. 2, p. 49–73.

Anderson, R. L., and Bancroft, T. A., 1952, Statistical theory in research: New York, McGraw-Hill Book Co., 399 p.

Antweiler, J. C., and Love, J. D., 1967, Gold-bearing sedimentary rocks in northwest Wyoming—A preliminary report: U.S. Geol. Survey Circ. 541, 12 p.

Baltz, E. H., 1967, Stratigraphy and regional tectonic implications of part of Upper Cretaceous and Tertiary rocks, east-central San Juan Basin, New Mexico: U.S. Geol. Survey Prof. Paper 552, 101 p.

Barghoorn, E. S., 1953, Evidence of climatic change in the geologic record of plant life [Chap.] 20, *in* Shapley, Harlow, ed., Climatic changes—evidence, causes, and effects: Cambridge, Mass., Harvard Univ. Press, p. 236–248.

Bell, K. G., and Hunt, J. M., 1963, Native bitumens associated with oil shales, Chap. 8, *in* Berger, I. A., ed., Organic geochemistry: New York, Macmillan Co., Internat. Ser. Mon. on Earth Sci., v. 16, p. 333–366.

Bradley, W. H., 1963, Paleolimnology, *in* Frey, D. G., ed., Limnology in North America: Madison, Wis., Univ. Wisconsin Press, p. 621–652.

Bradley, W. H., 1964, Geology of Green River Formation and associated Eocene rocks in southwestern Wyoming and adjacent parts of Colorado and Utah: U.S. Geol. Survey Prof. Paper 496–A, 86 p.

Bradley, W. H., and Eugster, H. P., 1969, Geochemistry and paleolimnology of the trona deposits and associated authigenic minerals of the Green River Formation of Wyoming: U.S. Geol. Survey Prof. Paper 496–B, 71 p.

Cashion, W. B., Jr., 1957, Stratigraphic relations and oil shale of the Green River Formation in the eastern Uinta Basin [Utah], *in* Intermtn. Assoc. Petroleum Geologists Guidebook 8th Ann. Field Conf., Uinta Basin: p. 131–135.

———1967, Geology and fuel resources of the Green River Formation, southeastern Uinta Basin, Utah and Colorado: U.S. Geol. Survey Prof. Paper 548, 48 p.

Chayes, Felix, 1960, On correlation between variables of constant sum: Jour. Geophys. Research, v. 65, no. 12, p. 4185–4193.

Coombs, D. S., Ellis, A. J., Fyfe, W. S., and Taylor, A. M., 1959, The zeolite facies, with comments on the interpretation of hydrothermal syntheses: Geochim. et Cosmochim. Acta, v. 17, p. 53–107.

Culbertson, W. C., 1964, Oil shale resources and stratigraphy of the Green River Formation in Wyoming: Mtn. Geologist, v. 1, no. 3, p. 181.

———1965, Tongues of the Green River and Wasatch Formations in southeastern part of the Green River Basin, Wyoming, *in* Wyoming Geol. Assoc. Guidebook, 19th Ann. Conf., Sedimentation of Late Cretaceous and Tertiary outcrops, Rock Springs uplift, 1965: p. 151–155.

———1969, Facies changes in the Eocene rocks in the southeastern part of the Green River basin, Wyoming, *in* Intermtn. Assoc. Geologists (and Utah Geol. Soc.) Guidebook 16th Ann. Field Conf., Uinta Mountains, Utah's maverick range: Salt Lake City, Utah, Utah Geol. Survey, p. 205–211.

Deer, W. A., Howie, R. A., and Zussman, J., 1962, Sheet silicates, v. 3 *of* Rock-forming minerals: New York, John

Denson, N. M., 1969, Distribution of nonopaque heavy minerals in Miocene and Pliocene rocks of central Wyoming and parts of adjacent States, *in* Geological Survey research 1969: U.S. Geol. Survey Prof. Paper 650–C, p. C25–C32.

Dobbin, E. C., Bowen, C. F., and Hoots, H. W., 1929, Geology and coal and oil resources of the Hanna and Carbon Basins, Carbon County, Wyoming: U.S. Geol. Survey Bull. 804, 84 p.

Donnell, J. R., 1961a, Tertiary geology and oil-shale resources of the Piceance Creek basin between Colorado and White Rivers, northwestern Colorado: U.S. Geol. Survey Bull. 1082–L, p. 835–891.

———1961b, Tripartition of the Wasatch formation near De Beque in northwestern Colorado, *in* Short papers in the geologic and hydrologic sciences: U.S. Geol. Survey Prof. Paper 424–B, p. B147–B148.

Dorr, J. A., Jr., 1952, Early Cenozoic stratigraphy and vertebrate paleontology of the Hoback Basin, Wyoming: Geol. Soc. America Bull., v. 63, no. 1, p. 59–93.

Evernden, J. F., Savage, D. E., Curtis, G. H., and James, G. T., 1964, Potassium-argon dates and the Cenozoic mammalian chronology of North America: Am. Jour. Sci., v. 262, no. 2, p. 145–198.

Fisher, D. J., Erdmann, C. E., and Reeside, J. B., Jr., 1960, Cretaceous and Tertiary formations of the Book Cliffs, Carbon, Emery, and Grand Counties, Utah, and Garfield and Mesa Counties, Colorado: U.S. Geol. Survey Prof. Paper 332, 80 p.

Fleischer, Michael, 1969, Additional data on rocks G–1 and W–1, 1965–1967, pt. 1 *of* U.S. Geological Survey standards: Geochim. et Cosmochim. Acta, v. 33, no. 1, p. 65–79.

Gazin, C. L., 1962, A further study of the lower Eocene mammalian faunas of southwestern Wyoming: Smithsonian Misc. Colln., v. 144, no. 1 (Smithsonian Inst. Pub. 4474), 98 p.

Gill, J. R., Merewether, E. A., and Cobban, W. A., 1970, Stratigraphy and nomenclature of some Upper Cretaceous and lower Tertiary rocks in south-central Wyoming: U.S. Geol. Survey Prof. Paper 667, 53 p.

Goddard, E. N., chm., and others, 1948, Rock-color chart: Washington, D.C., Natl. Research Council (repub. by Geol. Soc. America, 1951, 1971), 6 p.

Goldschmidt, V. M., 1954, Geochemistry [Alex Muir, ed.]: Oxford, Clarendon Press, 730 p.

Griffiths, J. C., 1966, A genetic model for the interpretive petrology of detrital sediments: Jour. Geology, v. 74, no. 5, pt. 2, p. 655–672.

Hardy, C. T., and Zeller, H. D., 1953, Geology of the west-central part of the Gunnison Plateau, Utah: Geol. Soc. America Bull., v. 64, no. 11, p. 1261–1278.

Harman, H. H., 1960, Modern factor analysis: Chicago, Univ. Chicago Press, 469 p.

Harshman, E. N., 1968, Geologic map of the Shirley Basin area, Albany, Carbon, Converse, and Natrona Counties, Wyoming: U.S. Geol. Survey Misc. Geol. Inv. Map I–539.

———1969, Wyoming uranium issue [spec. ed.] *of* Soc. Economic Geologists Field Conf., 1969: Wyoming Univ. Contr. Geology, v. 8, no. 2, pt. 1, p. 65–149.

Hawkins, J. W., Jr., and Whetten, J. T., 1969, Graywacke matrix minerals: Hydrothermal reactions with Columbia River sediments: Science, v. 166, p. 868–870.

Hay, R. L., 1966, Zeolites and zeolitic reactions in sedimen-

Henderson, G. V., 1958, Geology of the northeast quarter of the Soldier Summit quadrangle, Utah: Brigham Young Univ. Research Studies Geology Ser., v. 5, no. 5, 40 p.

Hite, R. J., and Dyni, J. R., 1967, Potential resources of dawsonite and nahcolite in the Piceance Creek basin, northwest Colorado: Colorado School Mines Quart., v. 62, no. 3, p. 25–38.

Hose, R. K., 1955, Geology of the Crazy Woman Creek area, Johnson County, Wyoming: U.S. Geol. Survey Bull. 1027–B, p. 33–118.

Imbrie, John, and VanAndel, T. H., 1964, Vector analysis of heavy-mineral data: Geol. Soc. America Bull., v. 75, no. 10, p. 1131–1156.

Johnson, R. B., 1959, Geology of the Huerfano Park area, Huerfano and Custer Counties, Colorado: U.S. Geol. Survey Bull. 1071–D, p. 87–119.

Johnson, R. B., Wood, G. H., Jr., and Harbour, R. L., 1958, Preliminary geologic map of the northern part of the Raton Mesa region and Huerfano Park in parts of Las Animas, Huerfano, and Custer Counties, Colorado: U.S. Geol. Survey Oil and Gas Inv. Map OM–183.

Keefer, W. R., 1957, Geology of the DuNoir area, Fremont County, Wyoming: U.S. Geol. Survey Prof. Paper 294–E, p. 155–221.

———1965, Stratigraphy and geologic history of the uppermost Cretaceous, Paleocene, and lower Eocene rocks in the Wind River Basin, Wyoming: U.S. Geol. Survey Prof. Paper 495–A, 77 p.

———1970, Structural geology of the Wind River Basin, Wyoming: U.S. Geol. Survey Prof. Paper 495–D, 35 p.

King, P. B., 1959, The evolution of North America: Princeton, N.J. Princeton Univ. Press, 189 p.

Knight, S. H., 1951, The Late Cretaceous-Tertiary history of the northern portion of the Hanna Basin, Carbon County, Wyoming, *in* Wyoming Geol. Assoc. Guidebook 6th Ann. Field Conf., south-central Wyoming: p. 45–53.

Krumbein, W. C., and Slack, H. A., 1956, Statistical analysis of low-level radioactivity of Pennsylvanian black fissile shale in Illinois: Geol. Soc. America Bull., v. 67, no. 6, p. 739–762.

Love, J. D., 1964, Uraniferous phosphatic lake beds of Eocene age in intermontane basins of Wyoming and Utah: U.S. Geol. Survey Prof. Paper 474–E, 66 p.

———1970, Cenozoic geology of the Granite Mountains area, central Wyoming: U.S. Geol. Survey Prof. Paper 495–C, 154 p.

Love, J. D., McGrew, P. O., and Thomas, H. D., 1963, Relationship of latest Cretaceous and Tertiary deposition and deformation to oil and gas in Wyoming, *in* Backbone of the Americas: Am. Assoc. Petroleum Geologists Mem. 2, p. 196–208.

Masursky, Harold, 1962, Uranium-bearing coal in the eastern part of the Red Desert area, Wyoming: U.S. Geol. Survey Bull. 1099–B, 152 p.

McGookey, D. P., 1960, Early Tertiary stratigraphy of part of central Utah: Am. Assoc. Petroleum Geologists Bull., v. 44, no. 5, p. 589–615.

McKenna, M. C., 1960, Fossil Mammalia from the early Wasatchian Four Mile fauna, Eocene of northwest Colorado: California Univ. Pubs. Geol. Sci., v. 37, no. 1, p. 1–130.

Miesch, A. T., Chao, E. C. T., and Cuttitta, Frank, 1966, Multivariate analysis of geochemical data on tektites: Jour. Geology, v. 74, no. 5, pt. 2, p. 673–691.

Muffler, L. J. P., and White, D. E., 1969, Active metamorphism of upper Cenozoic sediments in the Salton Sea geothermal field and the Salton trough, southeastern California: Geol. Soc. America Bull., v. 80, no. 2, p. 157–182.

Mullens, T. E., 1971, Reconnaissance study of the Wasatch, Evanston, and Echo Canyon Formations in part of northern Utah: U.S. Geol. Survey Bull. 1311–D, 131 p.

Myers, A. T., Havens, R. G., and Dunton, P. J., 1961, A spectrochemical method for the semiquantitative analysis of rocks, minerals, and ores: U.S. Geol. Survey Bull. 1084–I, p. 207–229.

Oil and Gas Journal, 1970, West Uinta seen as new "Red Wash freeway": Oil and Gas Jour., v. 68, no. 48, p. 91.

Olive, W. W., 1957, The Spotted Horse coalfield, Sheridan and Campbell Counties, Wyoming: U.S. Geol. Survey Bull. 1050, 83 p.

Olson, A. B., 1959, Photogeologic map of the Flat Top Mountain NE. quadrangle, Carbon County, Wyoming: U.S. Geol. Survey Misc. Geol. Inv. Map I–301.

Olson, J. S., and Potter, P. E., 1954, Statistical methods, pt. 1 *of* Variance components of cross-bedding direction in some basal Pennsylvanian sandstones of the Eastern Interior Basin: Jour. Geology, v. 62, no. 1, p. 26–49.

Oriel, S. S., 1961, Tongues of the Wasatch and Green River formations, Fort Hill area, Wyoming, *in* Short papers in the geologic and hydrologic sciences: U.S. Geol. Survey Prof. Paper 424–B, p. B151–B152.

———1962, Main body of Wasatch Formation near La Barge, Wyoming: Am. Assoc. Petroleum Geologists Bull., v. 46, no. 12, p. 2161–2173.

Oriel, S. S., and Tracey, J. I., Jr., 1970, Uppermost Cretaceous and Tertiary stratigraphy of Fossil basin, southwestern Wyoming: U.S. Geol. Survey Prof. Paper 635, 53 p.

Pettijohn, F. J., 1963, Chemical composition of sandstones—excluding carbonate and volcanic sands, chap. S. *of* Fleischer, Michael, ed., Data of geochemistry [6th ed.]: U.S. Geol. Survey Prof. Paper 440–S, p. S1–S21.

Privrasky, N. C., 1963, Geology of the Big Piney area, Sublette County, Wyoming: U.S. Geol. Survey Oil and Gas Inv. Map OM–205.

Rich, E. I., 1962, Reconnaissance geology of Hiland–Clarkson Hill area, Natrona County, Wyoming: U.S. Geol. Survey Bull. 1107–G, p. 447–540.

Robinson, Peter, 1957, Age of the Galisteo formation, Santa Fe County, New Mexico: Am. Assoc. Petroleum Geologists Bull., v. 41, no. 4, p. 757.

Roehler, H. W., 1965, Early Tertiary depositional environments in the Rock Springs uplift area, *in* Wyoming Geol. Assoc. Guidebook 19th Ann. Field Conf., Sedimentation of Late Cretaceous and Tertiary outcrops, Rock Springs uplift, 1965: p. 141–150.

———1970, Nonopaque heavy minerals from sandstone of Eocene age in the Washakie Basin, Wyoming, *in* Geological Survey research 1970: U.S. Geol. Survey Prof. Paper 700–D, p. D181–D187.

Rohrer, W. L., 1966, Geology of the Adam Weiss Peak quadrangle, Hot Springs and Park Counties, Wyoming: U.S. Geol. Survey Bull. 1241–A, 39 p.

Sears, J. D., and Bradley, W. H., 1924, Relations of the Wasatch and Green River formations in northwestern Colorado and southern Wyoming, with notes on oil shale in the Green River formation: U.S. Geol. Survey Prof. Paper 132, p. 93–107.

Shapiro, Leonard, 1967, Rapid analysis of rocks and minerals by a single-solution method, *in* Geological Survey research 1967: U.S. Geol. Survey Prof. Paper 575–B, p. B187–B191.

Sharp, W. N., 1970, Extensive zeolitization associated with hot springs in central Colorado, *in* Geological Survey research 1970: U.S. Geol. Survey Prof. Paper 700–B, p. B14–B20.

Sharp, W. N., McKay, E. J., McKeown, F. A., and White, A. M., 1964, Geology and uranium deposits of the Pumpkin Buttes area of the Powder River Basin, Wyoming: U.S. Geol. Survey Bull. 1107–H, p. 541–638.

Sheppard, R. A., and Gude, A. J., 3d, 1969, Diagenesis of tuffs in the Barstow Formation, Mud Hills, San Bernardino County, California: U.S. Geol. Survey Prof. Paper 634, 35 p.

Simpson, G. G., 1948, The Eocene of the San Juan Basin, New Mexico: Am. Jour. Sci., [pt. 1], v. 246, no. 5, p. 257–282; [pt. 2], v. 6, no. 6, p. 363–385.

Smith, J. W., and Milton, Charles, 1966, Dawsonite in the Green River Formation of Colorado: Econ. Geology, v. 61, no. 6, p. 1029–1042.

Snedecor, G. W., and Cochran, W. G., 1967, Statistical methods [6th ed.]: Ames, Iowa, Iowa State Univ. Press, 593 p.

Soister, P. E., 1968, Stratigraphy of the Wind River Formation in south-central Wind River Basin, Wyoming: U.S. Geol. Survey Prof. Paper 594–A, 50 p.

Stearns, C. E., 1943, The Galisteo formation of north-central New Mexico: Jour. Geology, v. 51, no. 5, p. 301–319.

Stephens, J. G., 1964, Geology and uranium deposits at Crooks Gap, Fremont County, Wyoming, *with a section on* Gravity and seismic studies in the Crooks Gap area, by D. L. Healey: U.S. Geol. Survey Bull. 1147–F, 80 p.

Stokes, W. L., and Madsen, J. H., Jr., compilers, 1961, Geologic map of Utah–northeast quarter: Utah Geol. and Mineralog. Survey.

Taylor, J. H., 1964, Some aspects of diagenesis: Adv. Sci., v. 21, p. 417–436.

Theobald, P. K., 1970, Preliminary geologic map of the north half of the Craig quadrangle, Moffat County, Colorado: U.S. Geol. Survey open-file rept.

Tourtelot, H. A., 1946, Tertiary stratigraphy in the northeastern part of the Wind River Basin, Wyoming: U.S. Geol. Survey Oil and Gas Inv. Prelim. Chart 22.

Tracey, J. I., Jr., Oriel, S. S., and Rubey, W. W., 1961, Diamictite facies of the Wasatch formation in the Fossil basin, southwestern Wyoming, *in* Short papers in the geologic and hydrologic sciences: U.S. Geol. Survey Prof. Paper 424–B, p. B149–B150.

Turekian, K. K., and Wedepohl, K. H., 1961, Distribution of the elements in some major units of the Earth's crust: Geol. Soc. America Bull., v. 72, no. 2, p. 175–192.

Van Houten, F. B., 1944, Stratigraphy of the Willwood and Tatman formations in northwestern Wyoming: Geol. Soc. America Bull., v. 55, no. 2, p. 165–210.

_____1948, Origin of red-banded early Cenozoic deposits in Rocky Mountain region: Am. Assoc. Petroleum Geologists Bull., v. 32, no. 11, p. 2083–2126.

Vine, J. D., 1969, Authigenic laumontite in arkosic rocks of Eocene age in the Spanish Peaks area, Las Animas County, Colorado, *in* Geological Survey research 1969: U.S. Geol. Survey Prof. Paper 650–D, p. D80–D83.

Vine, J. D., and Tourtelot, E. B., 1969, Geochemical investigations of some black shales and associated rocks: U.S. Geol. Survey Bull. 1314–A, p. A1–A43 [1970].

_____1970a, Preliminary geochemical and petrographic analysis of lower Eocene fluvial sandstones in the Rocky Mountain region, *in* Wyoming Geol. Assoc. Guidebook 22d Ann. Field Conf., Wyoming Sandstones Symposium: p. 251–263.

_____1970b, Geochemistry of black shale deposits—A summary report. Econ Geology, v. 65, no. 3, p. 253–272.

Walker, T. R., 1967, Formation of red beds in modern and ancient deserts: Geol. Soc. America Bull., v. 78, no. 3, p. 353–368.

Zeller, H. D., and Stephens, E. V., 1969, Geology of the Oregon Buttes area, Sweetwater, Sublette, and Fremont Counties, southwestern Wyoming: U.S. Geol. Survey Bull. 1256, 60 p.

U. S. GOVERNMENT PRINTING OFFICE : 1973 O - 490-247